

1 Cretaceous Research 133 (2022) 105137

2 <https://doi.org/10.1016/j.cretres.2022.105137>

3

4 **Late Cretaceous larger rovaliid Foraminifera from the westernmost Tethys**

5 Vicent Vicedo^{1,*} and Raquel Robles-Salcedo¹

6 ¹ Museu de Ciències Naturals de Barcelona, Departament de Paleontologia, Passeig

7 Picasso s/n, 08003 Barcelona, Spain.

8

9 * corresponding author: vvicedov@bcn.cat; vicent.vicedo@gmail.com

10

11 **Abstract**

12 A detailed taxonomical study of the larger rovaliid foraminifera found in the Upper
13 Cretaceous deposits from the External Prebetic Zones (SE Spain) has been carried out
14 for the first time. The study of the samples has revealed the diversity and abundance of
15 this foraminiferal group and its usefulness as a tool for regional biostratigraphy. Five
16 new species and two new genera are described, *Pseudosulcoperculina bocairentina* gen.
17 et sp. nov., *Plumopraelockhartia solanensis* gen. et sp. nov., *Rotalia baetica* sp. nov.,
18 *Suturina minima* sp. nov., and *Neorotalia? pinetensis* sp. nov. These and other species
19 of larger benthic foraminifera have been found forming two different assemblages. The
20 older assemblage, dated as middle to late Campanian, is composed of the rovaliid
21 species *N.? pinetensis* sp. nov., *R. baetica* sp. nov., *Suturina globosa*, *Rotorbinella* sp.,
22 *Pararotalia tuberculifera* and *Rotalispira scarsellai*. The younger assemblage is dated

23 as late Maastrichtian, including the rotaliids *Pseudosulcoperculina bocairentina* gen. et
24 sp. nov., *Plumopraelockhartia solanensis* gen. et sp. nov. and *Pararotalia tuberculifera*.
25 In global terms, the Late Cretaceous rotaliids from the Prebetic are key in our
26 understanding of the phylogenetic relationships among the Cretaceous and early
27 Paleocene Tethyan species, allowing to root the origin of the lockhartiines sensu lato
28 back to the Upper Cretaceous. Besides, the new data regarding the *Sulcoperculina*-like
29 forms have revealed the differences and similarities among the species of both sides of
30 the Atlantic, especially, between the architecture of the American genus *Sulcoperculina*
31 and that of similar forms in Pyrenean and Tethyan realms, grouped into new a genus
32 here introduced as *Pseudosulcoperculina*.

33 **Keywords.** Foraminifera, Rotaliidae, Prebetic, Cretaceous, Tethys, biostratigraphy.

34

35 **1. Introduction**

36 The major extinction at the end of Cenomanian extinguished all the k-strategic benthic
37 foraminifera and left the shallow marine ecosystems available to be potentially
38 colonized by other upcoming benthic communities (Raup and Sepkoski, 1986; Caus et
39 al., 1993, 1997; Kaiho and Hasegawa, 1994; Silva and Sliter, 1999; Leckie et al., 2002;
40 Hart et al., 2005; Parente et al., 2007, 2008; Consorti et al., 2015; Arriaga, 2016, among
41 others). The group of larger foraminifers with lamellar-perforated (hyaline) tests, scarce
42 in the Cenomanian times, took this opportunity, spreading and diversifying during the
43 Coniacian to Maastrichtian ages. In the Iberian Peninsula, the Pyrenean basin is
44 considered a hotspot for this and other biotic groups during post-Turonian times. The
45 shallow-water carbonate successions deposited in this area contain rich assemblages of
46 hyaline larger foraminifera, which have been the subject of many studies, especially in

47 the two last decades (Boix et al., 2009, 2011; Robles-Salcedo et al., 2013, 2018, 2019;
48 Albrich et al., 2014, 2015; Caus et al., 2016; Consorti et al., 2017a, b; Villalonga et al.,
49 2019, among many others). Among the lamellar-perforate foraminifera, the vast group
50 of larger rotaliids, referring to representatives of the Rotaliidae *sensu stricto* as well as
51 other closely related rotaliform taxa not strictly in this family, can be considered
52 particularly successful as they not only diversified in terms of morphology but also
53 colonized several types of shallow-water environments (Boix et al., 2009; Consorti et
54 al., 2017a, b; Hottinger, 2014; Vicedo et al., 2019).

55 The abundance and diversity of larger rotaliids in the Late Cretaceous are the main
56 factors that make them of interest for biostratigraphy. Nonetheless, to improve our
57 understanding of the phylogenetic relationships, evolutionary patterns and
58 biostratigraphical significance of rotaliids in global terms, as in any other group of
59 larger foraminifers, it is essential to undertake architectural analysis of the poorly
60 studied populations. This is the case of the larger rotaliids of the Betic margin, the
61 western area of the Tethyan domain.

62 The aim of the present study is precisely to update a taxonomic revision of the
63 aforementioned group. To this end, several stratigraphic series in the northeastern
64 foothills of the External Prebetic Zones in the Iberian Peninsula have been sampled and
65 their micropalaeontological content analysed with taxonomical, biostratigraphical and
66 palaeobiogeographical approaches.

67

68 **2. Geological and geographical settings**

69 The Betic System, or Betic Cordillera, is one of the major mountain ranges located in
70 the southern and eastern part of the Iberian Peninsula. It can be subdivided into the
71 Internal and External Zones, which have different geological and topographical features.
72 The Internal Zones, or Penibetic System, is composed of several tectono-sedimentary
73 complexes including the basement and the sedimentary cover comprising the highest
74 elevations. The External Zones, which are subdivided into Prebetic and Subbetic
75 Systems, are composed of sedimentary rocks from Triassic to Miocene ages (Azañón et
76 al., 2002; Vera, 2004, and references therein).

77 During Cretaceous times, the External Prebetic Zones formed the passive southern
78 margin of the Iberian plate, and these are composed of a complex system of continental
79 to outer platform environments, which developed in the context of regional rifting
80 episode. The deposits accumulated in these environments consist of carbonates and
81 clastics (Fourcade, 1970; Azema et al., 1979; Vera et al., 1982; Martín-Chivelet, 1996;
82 Azañón et al., 2002; Vilas et al., 2003, among others).

83

84 **3. Material and methods**

85 To carry out this study, we sampled a total of four stratigraphic logs from the south of
86 Valencia province, Spain (eastern Iberian Peninsula), namely, Serra de la Solana, Serra
87 Grossa, Penya del Romaní and Serra de les Agulles sections. In addition, we also
88 sampled two other isolated stratigraphic levels from other areas of the Iberian Peninsula
89 that contain similar larger foraminifera assemblages (Fig. 1). One of them is from an
90 outcrop also located in the Prebetic domain but in another sector, in the Sierra del
91 Regalí near the village of Letur (Albacete, Spain). The other is from the locality of La
92 Tosa near the village of Tremp (Lleida, Spain) in the Southern Pyrenees. We have

93 included these two isolated samples for comparison purposes, given their relevance in
94 terms of paleobiogeography.

95 As many as 242 samples were collected and up to 700 thin sections of rocks were taken
96 to carry out the micropalaeontological study. All the samples and thin-sections are
97 housed under the acronym MGB in the collections of the Department of Palaeontology,
98 Museu de Ciències Naturals de Barcelona (see Supplementary material).

99 We refer to Hottinger (2006, 2014) and Vicedo et al. (2019) for the definition of
100 architectural terms in the systematic chapter.

101 Manuscript Zoobank ID

102 LSID urn:lsid:zoobank.org:pub:2916CF87-93BE-48EC-8334-6A171580E30C

103 **Description of the stratigraphic sections**

104 **Serra de la Solana section.** UTM coordinates (ETRS89, H30) are: X: 705.611,35;
105 Coord. Y: 4.292.919,06 (bottom) and X: 705.327,82; Coord. Y: 4.292.821,58 (top) (Fig.
106 2). This section was measured to the north-west of the village of Bocairent (Valencia,
107 Spain), in a small mountain system called Serra de la Solana. In this area, the Upper
108 Cretaceous succession is around 500 m thick (according to the IGME map 820
109 *Onteniente*) consisting of carbonates deposited in a shallow-water platform. The
110 deposits, that encompass from the Cenomanian to the Maastrichtian ages, are strongly
111 affected by dolomitization resulting in an alternation of dolomites, dolomitic
112 limestones, bioclastic limestones and sandy limestones. At the top, the Maastrichtian is
113 truncated by a discontinuity, overlying by limestone deposits of Miocene age. The
114 sampling was carried out in a composite section about 80 m thick corresponding to the
115 uppermost Cretaceous deposits, paying special attention to the last few meters of the

116 sucession, in an interval dated Maastrichtian in age by Pons et al. (1994) and Granero et
117 al. (2018). The interval sampled, was selected because of its relatively rich fossil
118 assemblages, among which the hyaline larger benthic foraminifera (LBF) are
119 abundantly represented. Further details concerning the sampling performed and the
120 characteristics of fossil assemblages found in this stratigraphic interval can be found in
121 Granero et al. (2018). The uppermost Cretaceous succession in this area has been
122 lithostatigraphically controversial as it has been named in many ways. Vera et al. (1982)
123 considered the succession as belonging to the Mariasnal formation (Fm). In the current
124 geological maps provided by the Instituto Geológico y Minero de España (IGME) (see
125 <http://info.igme.es/visorweb/>) it is referred from bottom to top as Sierra de la Solana
126 (Vera et al., 1982) and Calizas de Carche formations (Fms) (Martín-Chivelet, 1994).
127 Considering the lithostratigraphical units defined for the sector Onteniente-Denia by
128 Martín-Chivelet and Chacón (2004), the interval studied in the present paper could be
129 ascribed to the Calizas Arenosas del Molar Fm (Martín-Chivelet, 1994) (see Fig. 2).

130 **Serra Grossa section.** UTM coordinates (ETRS89, H30) are: X: 704.123,35; Y:
131 4.302.446,50 (bottom) and X: 704.196,88; Y: 4.302.054,54 (top) (Fig. 3). This section
132 is located to the north-west of the village of Ontinyent (Valencia, Spain), in a mountain
133 range called Serra Grossa. In this locality, the Upper Cretaceous series is around 400 m
134 thick (according to IGME map 820 *Onteniente*), consisting mainly of dolomites,
135 dolomitic limestones and limestones, with occasional sandy intercalations. The samples
136 were collected along the CV-665 road in an approximately 100m thick stratigraphical
137 section, corresponding mainly to limestones and dolomitic limestones which are rich in
138 larger foraminifera. From bottom to top, the interval studied has been identified [as](#)
139 belonging, from bottom to top, to the Calizas de la Sierra Utiel and Margas de los
140 Cerrillares Fms (Martín-Chivelet, 1994) dated as Coniacian to Maastrichtian according

141 to the IGME maps. However, following the nomenclature of Martín-Chivelet and
142 Chacón (2004) the interval studied in the present paper could be considered as
143 belonging to the Calizas de la Rambla de los Gavilanes Fm (Martín-Chivelet, 1994)
144 (Fig. 3).

145

146 **Penya del Romaní section.** The UTM coordinates (ETRS89, H30) are: X: 731.117,41;
147 Y: 4.318.871,69 (bottom) and X: 730.894,63; Y: 4.318.542,62 (top) (Fig. 4). This
148 section was logged to the north-east of the village of Pinet (Valencia, Spain), between
149 Les Mamelles and Penya del Romaní hills. Here, the interval of the Upper Cretaceous
150 series sampled consists of around 150 m of fossiliferous shallow-water limestones
151 intercalated with marly clays, sandy limestones, sandstones, microconglomerates and
152 dolomites. The interval studied encompasses materials belonging to Rambla de los
153 Gavilanes Fm at the bottom, and probably Calizas Arenosas del Molar Fm at the top,
154 according to the IGME geological map 1:50.000 (see in <http://info.igme.es/visorweb/>).
155 On the basis of the larger foraminifera assemblages found, the interval studied was
156 recently dated as late Campanian (Robles-Salcedo and Vicedo, 2016).

157 **Serra de les Agulles section.** The UTM coordinates (ETRS89, H30) are: X: 732.297;
158 Y: 4.330.168 (bottom) and X: 732.229; Y: 4.330.297 (top) (Fig. 5). The section is found
159 to the north-east of the village of Tavernes de la Valldigna (Valencia, Spain, see Robles-
160 Salcedo, 2014, for the log location). The interval studied consists of a 70m thick layer
161 fossiliferous limestones intercalated with marly clays, sandy limestones,
162 microconglomerates and rudist limestones, belonging from bottom to top to the Calizas
163 de la Rambla de los Gavilanes Fm, according to the IGME geological map 1:50,000

164 (see in <http://info.igme.es/visorweb/>). This interval is dated as Campanian to
165 Maastrichtian in age (Eckstaller, 1993; Pons and Vicens, 2002).

166 **Serra del Regalí and La Tosa outcrops.** Similar Upper Cretaceous larger foraminifera
167 assemblages were found in two isolated samples at our disposal collected in the
168 localities of Serra del Regalí (Albacete, Spain) and La Tosa (Lleida, Spain). The former
169 has been included because of its proximity to the areas studied, belonging to the
170 Prebetic of Albacete. The latter outcrop is located in the Pyrenean Basin, but it has been
171 considered essential to include it in the present study because of the relevance of its
172 larger foraminiferal content, this being useful in later phylogenetical and
173 palaeobiogeographical discussions.

174 The outcrop of Serra del Regalí consists of a succession of limestones, occasionally
175 dolomites, calcarenites and marls belonging to Serra de Utiel Fm. according to the
176 IGME geological map 1:50,000 (see in <http://info.igme.es/visorweb/>). The stratigraphic
177 level studied is located close to the village of Letur (Albacete, Spain). UTM coordinates
178 (ETRS89, H30) are: X: 582.399.25; Y: 4.248.312,43.

179 The outcrop of La Tosa consists of a succession of calcarenites, limestones and marls
180 belonging to the lower unit of the Arén Sandstone Fm (for more information see
181 Robles-Salcedo, 2014; Caus et al., 2016; Robles-Salcedo et al., 2018). La Tosa is
182 located a few kilometers to the north of the village of Tremp (Lleida, Spain). UTM
183 coordinates (ETRS89, H31) are: X: 328.666,73; Y: 4.673.827,41.

184

185 **4. Systematic descriptions**

186

187 Phylum **Foraminifera** d'Orbigny, 1826

188 Class **Globothalamea** Pawlowski, Holzmann and Tyszka, 2013

189 Subclass **Rotaliana** Mikhalevich, 1980

190 Order **Rotaliida** Delage and Hérouard, 1896

191 Superfamily **Rotalioidea** Ehrenberg, 1839

192 Family **Rotaliidae** Ehrenberg, 1839

193 Genus ***Pseudosulcoperculina*** gen. nov.

194 LSID urn:lsid:zoobank.org:act:0FB6A4B6-999C-4967-BB7B-66CF7A4978E8

195 **Type species.** *Pseudosulcoperculina bocairentina* gen. et sp. nov.

196 **Etymology.** *Pseudo-*, latin word of "false", has been given due to the resemblance to
197 specimens ascribed to the genus *Sulcoperculina*.

198 **Diagnosis.** Lamellar-perforated test with trochospiral chamber arrangement. Shell-
199 shape lenticular to subglobular, involute growth in both, ventral and dorsal sides. Dorsal
200 side smooth to slightly ornamented by beads. Ventral chamber wall feathered. Margin
201 showing a deep fold or sulcus formed by a peripheral invagination of the wall. Sulcus
202 wall showing a distinctive ornamentation based on multiple indentations. One single
203 intraseptal canal connected to the sulcus. Umbilical structure of the ventral side
204 composed of a spiral umbilical canal limited by an umbilical plate extending over the
205 ventral surface of the chamber and covering the feathered grooves. Umbilicus composed
206 of a central massive structure or umbo pierced peripherally by narrow funnels. Simple
207 aperture consisting of a narrow slit in interiomarginal position.

208 **Differences and similarities.** *Pseudosulcoperculina* gen. nov. has a distinctive
209 sulcoperculina-like morphology. Its characteristic marginal sulcus is quite similar to that
210 of the genus *Sulcoperculina* Thalmann, 1939, typical from the Upper Cretaceous
211 deposits of the American-Caribbean paleobioprovince. Although the shell-architecture
212 of the latter has been very controversial since its description, which hamper later
213 comparisons (see remarks below), the revision of the specimens of the type species *S.*
214 *dickersoni* (Palmer, 1934) published in the original paper has allowed us to identify the
215 main architectural differences between our morphotype and the genus *Sulcoperculina*.
216 The main differences are the bilateral symmetry of *S. dickersoni* versus de trochospiral
217 assymmetric test of *P. bocairentina* gen. et sp. nov., and the presence of some kind of
218 marginal canal system in the former versus the absence of such structure in the latter.
219 The architecture of *Pseudosulcoperculina* gen. nov. is different from the other
220 Cretaceous rotaliid genera by the presence of the following structures in the same form:
221 the marginal sulcus plus the ventral feathered structure.

222 *Pseudosulcoperculina bocairentina* gen. et sp. nov.

223 (Figures 6, 7, 8A–E)

224 1994 *Sulcoperculina dickersoni* (Palmer) var. *vermunti* (Thiadens); Ramírez del Pozo
225 and Martín-Chivelet: pl. 3, fig. 5

226 2018 Rotaliidae indet.; Granero et al.: fig 11F–G

227 LSID urn:lsid:zoobank.org:act:2C546F64-291F-4CFC-9E6F-58720F455F88

228 **Etymology.** *bocairentina* is the female demonym of Bocairent, the village in which the
229 type locality is found.

230 **Types.** The holotype is MGB 69778 LP05.005 (Fig. 6F). The other specimens
231 illustrated in Figures 6 and 7 are paratypes.

232 **Type horizon and locality.** Calizas Arenosas del Molar Fm, upper Maastrichtian, Serra
233 de la Solana, Bocairent (Valencia, Spain).

234 **Diagnosis.** Lamellar-perforated test with thick wall and trochospiral chamber
235 arrangement. Dorsal and ventral sides involute. Shell-shape lenticular to subglobular.
236 Acute margin showing a characteristic deep groove or sulcus. Ventral chamber wall
237 feathered. Umbilical structure composed of a central umbo. Simple aperture consisting
238 of a narrow slit in interiomarginal position. Intraseptal and spiral interocular spaces or
239 canals connected and opening into the sulcus. Shell with a diameter of around 1 mm and
240 three whorls; variable proloculus, of around 50–110 μm .

241 **Description.** The surface of the dorsal side is smooth to slightly ornamented with beads,
242 the ventral side is dominated by feathered ornamentation and a marked umbo. The
243 peripheral margin is acute and asymmetric, showing a deep groove running in the
244 direction of growth, parallel to the periphery and slightly displaced towards the ventral
245 part of the shell. The spiral interocular space is narrow, being separated from the
246 chamber lumen by the umbilical plate and connected to the intraseptal interocular
247 spaces. Vertical umbilical canals or funnels connect the spiral interocular space to the
248 exterior. Several grooves run parallel from the intraseptal interocular space to the
249 chamber shoulder of the ventral side developing the feathered ornamentation. The
250 intraseptal interocular spaces or canals open into the sulcus through marginal openings.
251 The shell has a maximum diameter of around 1 mm and 3 complete whorls, with around
252 20 chambers in the last whorl. The proloculus is spherical to subspherical, with a

253 diameter that varies from 35 to 60 μm . The central part of the shell is occupied by a
254 solid umbilical mass.

255 **Differences and similarities.** Some morphological traits of *Pseudosulcoperculina*
256 *bocairentina* gen. et sp. nov. are similar to those of the type species *Sulcoperculina*
257 *dickersoni* (Palmer, 1934) from the Upper Cretaceous of Cuba, especially by their
258 marginal groove. However, the former has an asymmetric shell and the latter is clearly a
259 biumbilicate species with bilateral symmetry. The same differences can be noted when
260 comparing *Pseudosulcoperculina bocairentina* sp. nov. with the other species of the *S.*
261 *gr. dickersoni*. *Pseudosulcoperculina bocairentina* gen. et sp. nov. also differs from *S.*
262 *gr. dickersoni* in having a marked feathered ornamentation in the ventral chamber wall.
263 On the other hand, the asymmetry of the shell and the marked feathered ornamentation
264 of the new species are similar to those of *S. kugleri*. *Pseudosulcoperculina bocairentina*
265 gen. et sp. nov. differs from *S. kugleri* in having a thinner wall and higher trochospire.

266 Regarding the Prebetic domain, we have also identified *P. bocairentina* gen. et sp. nov.
267 in some isolated samples collected in the Maastrichtian deposits from the *Sierra del*
268 *Regalí* (Albacete, Spain) (Figs. 8A–E). The specimen identified as *S. dickersoni*
269 (Palmer) var. *vermunti* (Thiadens) by Ramírez del Pozo and Martín-Chivelet (1994, pl.
270 3, Fig. 5) found in equivalent deposits from the Maastrichtian of Sierra Larga (Murcia,
271 Spain) should, in our opinion, also be ascribed to the species *P. bocairentina* sp. nov.

272 A closely related form to *P. bocairentina* gen. et sp. nov. has been observed in the lower
273 Maastrichtian of the southern Pyrenees, in a locality called *La Tosa* (Fig. 9). The
274 marginal sulcus seems to be less developed, but the feathered ornamentation is present.
275 Due to the scarcity of material, we have been unable to identify it to species level,
276 leaving this morphotype in open nomenclature as *Pseudosulcoperculina* sp.

277 Nonetheless, given its smaller proloculus and less developed marginal sulcus, we
278 consider it likely that this morphotype will be defined as a new species in future studies,
279 with new material. The LBF association found together with *Pseudosulcoperculina* sp.
280 in *La Tosa* consists of *Dictypsella* sp., *Haddonina* sp., *Nummofallotia cretacea*
281 (Schlumberger, 1900), *Fascispira colomi* Silvestri, 1940, undetermined species in the
282 Fabularidae family, *Praestorrsella roestae* (Visser, 1951), *Linaresia* sp., *Pararotalia*
283 *tuberculifera* (Reuss, 1862), *Pyrenorotalia* sp., *Lepidorbitoides socialis* (Leymerie,
284 1851), *Orbitoides gruenbachensis* Papp, 1955, *O. aff. concavatus* Rahaghi, 1976, and
285 *Siderolites pyrenaicus* Robles-Salcedo, Vicedo and Caus, 2018.

286 Other forms with a certain resemblance to *Pseudosulcoperculina bocairentina* gen. et
287 sp. nov. have been observed in the Santonian–Campanian deposits outcropping close to
288 the locality of Tragó de Noguera, southern Pyrenees (see Hottinger, 1966) and in the
289 Santonian (?)–Campanian strata of Murge, Italy (see p. 594–595 in Luperto Sinni and
290 Ricchetti, 1978). Nevertheless, there are some morphological differences among all
291 these morphotypes. The Campanian *Sulcoperculina* specimens figured in Fig. 10C, D
292 and Fig. 11A–E in Hottinger (1966) are architecturally closer to primitive Siderolitidae
293 Finlay, 1939, than to *Sulcoperculina*, as previously pointed out by Wannier (1983). The
294 only specimen that could be considered close to *Sulcoperculina* is the specimen
295 illustrated in Fig. 10E (op. cit.) cited as *Sulcoperculina aff. cubensis* (Palmer) from the
296 Santonian of the Montsec Mountains. On the other hand, the specimens of Luperto
297 Sinni and Ricchetti (1978) cited as *Sulcoperculina* sp. seem to lack the sulcus and the
298 feathered ventral ornamentation. More material is needed to confirm the generic and
299 specific identification of all these morphotypes.

300 The feathered ornamentation, lenticular morphology and solid mass or umbo make the
301 architecture of *P. bocairentina* sp. nov. somewhat similar to that of the representatives

302 of the subfamily Kathiniinae Hottinger, 2014, specially the group of elazigines.
303 Nonetheless, the presence of a marked marginal sulcus, the canal system and the
304 involute dorsal side in the former allows its differentiation from all Kathiniinae.
305 The morphotype identified as *Sulcoperculina globosa?* in Butterlin (1967) from the
306 upper Maastrichtian of Greece seems to be different from *P. bocairentina* gen. et sp.
307 nov. by the absence of a peripheral sulcus, which would permit also to remove it from
308 the genus *Sulcoperculina*.

309 Subfamily **Praelockhartiinae** Vicedo and Robles-Salcedo, 2019

310 Genus *Plumopraelockhartia* gen. nov.

311 LSID urn:lsid:zoobank.org:act:AFBE0391-8775-4367-9722-344023E1CBC1

312 **Type species.** *Plumopraelockhartia solanensis* sp. nov.

313 **Etymology.** From *pluma*, the Latin name for feather, referring to the feathering ventral
314 ornamentation, and *Praelockhartia*, the genus which shows architectural similarities.

315 **Diagnosis.** Lamellar-perforated test, trochospiral chamber arrangement and subacute
316 periphery. Dorsal side evolute, surface smooth to slightly ornamented with beads.
317 Ventral side involute with an umbilicus composed of foliar piles and funnels; chamber-
318 wall surface feathered. The umbilical structure is composed of interpile and peripheral
319 cavities, the latter produced by proximal folium folding. Aperture simple.

320 **Differences and similarities.** The architecture of the type species of the new genus,
321 *Plumopraelockhartia solanensis* gen. et sp. nov., is reminiscent of that of the
322 representatives of the Paleogene subfamilies Praelockhartiinae Vicedo and Robles-
323 Salcedo, 2019, and Lockhartiinae Hottinger, 2014, due to its umbilical cavities;

324 however, the fact that these cavities are less developed and more irregularly arranged in
325 the new genus suggest that this should be better ascribed to the subfamily
326 Praelockhartiinae. Actually, the basic architecture of the new genus
327 *Plumopraelockhartia* is very close to that of *Praelockhartia* Vicedo and Robles-
328 Salcedo, 2019, from the Danian of Oman, the latter differing from the former mainly in
329 its rounded periphery, its coarsely perforated wall, the absence of dorsal ornamentation
330 consisting of more marked beads and the absence of ventral feathered ornamentation.
331 The feathered ornamentation and the coarsely perforated wall are also absent in other
332 genera considered in Vicedo et al. 2019 as belonging to the Praelockhartiinae, such as
333 *Rotospirella* Hottinger, 2014, *Rotalispira* Hottinger, 2014, and *Rotalispirella* Consorti
334 et al., 2017b. These last three genera also differ from *Plumopraelockhartia* in having
335 thinner and more delicate folia. In addition, *Rotalispira* and *Rotalispirella* have less
336 developed piles and *Rotospirella* has less developed interpile cavities.

337 The feathered ornamentation of *Plumopraelockhartia* is similar to that exhibited by the
338 species ascribed to the Paleogene genus *Elazigina* Sirel, 2012, type species *E.*
339 *subsphaerica* (Sirel, 1972). There are marked differences in the umbilical structure,
340 however, these allowing its differentiation at generic and even at subfamily level.

341 Other Cretaceous rotaliid genera defined up to now in the literature show dissimilar
342 architectures, lacking the umbilical cavities typical from the praelockhartiines. This
343 umbilical structures are one of the most diagnostic features that differentiates the new
344 genus *Plumopraelokhartia* from other Cretaceous rotaliids known so far.

345 *Plumopraelockhartia solanensis* gen. et sp. nov.

346 (Figures 8F–G, 10)

347 LSID urn:lsid:zoobank.org:act:23AE2E67-E247-4B51-B65E-731EBBBC88BF

348 **Etymology.** From the type locality of Sierra de la Solana.

349 **Types.** The holotype is MGB 84627 LP01.004 (Fig. 10B). The other specimens
350 illustrated in Figure 10 are paratypes.

351 **Type horizon and locality.** Calizas Arenosas del Molar Fm, Maastrichtian, Serra de la
352 Solana, Bocairent (Valencia, Spain).

353 **Diagnosis.** Lamellar-perforated test with trochospiral chamber arrangement. Dorsal side
354 evolute and smooth to slightly ornamented with beads. Ventral side involute and
355 feathered. Shell-shape lenticular with acute margin. Simple aperture in interiomarginal
356 position. Umbilical structure composed of several piles. Interpile umbilical cavities
357 occupying the tubular, vertical spaces among piles. Umbilical peripheral cavities located
358 towards the periphery of the umbilicus. Shell has a diameter of around 0.8 mm and 2.5
359 whorls; proloculus of about 30 μm .

360 **Description.** The dorsal side is smooth to slightly ornamented with beads. The ventral
361 side is dominated by feathered ornamentation, consisting of numerous parallel grooves
362 extending in a perpendicular direction from suture onto chamber shoulders. The
363 umbilical structure is typically composed of several foliar piles and funnels. The
364 interpile umbilical cavities are irregular and located in the vertical umbilical spaces. The
365 folia posterior folding or indentation produces the peripheral umbilical cavities. The
366 shell has a diameter of 0.5 to 0.8 mm and around 2 to 2.5 whorls, with about 12–13
367 chambers in the last whorl. The proloculus is spherical to subspherical showing a
368 diameter that varies from 25 to 30 μm .

369 **Differences and similarities.** The species *Elazigina siderea* Consorti and Rashidi,
370 2018, from the Maastrichtian of the Tarbur Formation, Iran, is similar to
371 *Plumopraelockhartia solanensis* gen. et sp. nov. in having feathered ornamentation and

372 isolated umbilical piles. The main architectural difference between the two species is
373 related to the umbilical structure. *Plumopraelockhartia solanensis* gen. et sp. nov.
374 shows peripheral and interpile umbilical cavities, while *Elazigina siderea* has a central
375 massive plug surrounded by secondary piles and a complex umbilical canal system.
376 Besides, concerning this last species, the comparison of the specimens of *E. siderea*
377 illustrated in Consorti and Rashidi (2018) with those of the type species of *Elazigina*,
378 the Paleocene *E. subsphaerica* (Sirel, 1972) allows distinguishing a very different
379 umbilical structure. The former has a central plug surrounded by a complex umbilical
380 canal system and the latter shows a more massive umbilical structure. This clarification,
381 which warrants a reanalysis of the complex umbilical architecture of *E. siderea*, would
382 be crucial to reevaluate its generic ascription as well as the early evolution of the whole
383 group of kathinines in the Tethyan domain.

384 *Smoutina cruysi* Drooger, 1960, the type species of the genus *Smoutina* Drooger, 1960,
385 from the Upper Cretaceous deposits of the Atlantic-Caribbean palaeobioprovince differs
386 from *P. solanensis* gen. et sp. nov. in lacking an umbilical plate and in having multiple
387 and simple funnels.

388 Genus ***Rotalispira*** Hottinger, 2014

389 **Type species.** *Rotorbinella scarsellai* Torre, 1967.

390 ***Rotalispira scarsellai*** (Torre, 1967)

391 (Figure 11)

392 1967 *Rotorbinella scarsellai* n. sp.; Torre: p. 422, pl. 1, figs 1–8, pl. 2, Fig. 10.

393 1972 *Rotorbinella scarsellai* Torre; Bignot: pl. VII, fig. 6.

- 394 1976 *Rotorbinella scarsellai* Torre; Luperto Sinni: pl. 52, figs 1–5.
- 395 1976 *Rotorbinella* sp.; Luperto Sinni: pl. 52, figs 6, 7.
- 396 1976 *Stomatorbina?* sp.; Luperto Sinni: pl. 53, figs 8–10.
- 397 1976 *Coleites?* sp.; Luperto Sinni: pl. 53, fig. 11.
- 398 1978 *Rotorbinella scarsellai* Torre; Luperto Sinni and Ricchetti: pl.62, figs 5, 6.
- 399 1978 *Stomatorbina?* sp.; Luperto Sinni and Ricchetti: pl. 62, figs12–14.
- 400 1978 *Stensioeina surrentina* Torre; Luperto Sinni and Ricchetti: pl.62, fig 11.
- 401 1994 *Rotorbinella scarsellai* Torre; Chiocchini et al.: pl. 22, figs6,7,14,15.
- 402 2007 *Rotorbinella scarsellai* Torre; Tentor: fig 7C.
- 403 2008 *Rotorbinella scarsellai* Torre; Chiocchini et al.: pl. 30, fig 1.
- 404 2008 *Stensioeina surrentina* Torre; Schlüter et al.: fig 4G.
- 405 2012 *Rotorbinella scarsellai* Torre; Chiocchini et al.: pl. 132, figs 1–8.
- 406 2014 *Rotalispira scarsellai* (Torre); Hottinger: pl. 5.1.
- 407 2015 *Rotorbinella scarsellai* Torre; Frijia et al.: fig 8G.
- 408 2017 *Rotalispira scarsellai* (Torre); Solak et al.: fig 11I.
- 409 2017 *Stensioeina surrentina* Torre; Solak et al.: fig 11O, P.
- 410 2017a *Rotalispira scarsellai* (Torre); Consorti et al.: fig 6M.
- 411 **Description.** The shell is lamellar perforated with biconvex morphology, keeled
- 412 periphery and trochospiral chamber arrangement. The dorsal side is evolute, showing

413 rich ornamentation mainly based on limbate sutures. The proloculus is around 36–60
414 µm. The foramen consists of a slit in an interiomarginal position. The umbilical plate
415 separates the main chamber lumen from the foliar chamberlet. The foliar apertures
416 connect the subsequent foliar chamberlets forming a kind of spiral canal. The umbilical
417 structure is composed of large folia and slender umbilical piles.

418

419 Subfamily **Rotaliinae** Ehrenberg, 1839

420 Genus **Rotalia** Lamarck, 1804

421 Type species *Rotalites trochidiformis* Lamarck, 1804

422 ***Rotalia baetica*** sp. nov.

423 (Figure 12)

424 LSID urn:lsid:zoobank.org:act:EAF36C4D-D8B3-4A86-8336-A0CCEAFBEC9A

425 **Etymology.** From the Latin word *Baetica*, which was an ancient Roman province and is
426 the current name given to the Cordillera of southeastern Spain.

427 **Types.** The holotype is MGB 60323 LP03.007 (Fig. 12E). The other specimens
428 illustrated in Figure 10 are paratypes.

429 **Type horizon and locality.** Calizas de la Rambla de los Gavilanes Fm, upper
430 Campanian, *Penya del Romaní Hill* (Pinet, Valencia, Spain).

431 **Diagnosis.** Lamellar-perforated test with low-trochospiral chamber arrangement and
432 keeled periphery. Lenticular, biconcave shell. Aperture simple in an interiomarginal
433 position. Dorsal side evolute, smooth or with slight ornamentation. Ventral side flat to
434 slightly convex. Umbilical structure of fused folia forming a columella. Megalospheric

435 forms with a proloculus of around 26 μm , maximum diameter of adult shells of around
436 1 mm and a height of about 0.5 mm with four whorls. No microspheric forms identified.

437 **Differences and similarities.** The adult forms of the type species *Rotalia trochidiformis*
438 (Lamarck) are smaller and with a dorsal side more concave. The scarce specimens of
439 *Rotalia baetica* sp. nov. found seem to resemble, on first inspection, those of the
440 megalospheric generation of *Iberorotalia reicheli* (Hottinger, 1966) from the lower
441 Santonian of the southern Pyrenees, especially in having an acute margin; but the
442 umbilical structure is different in the two morphotypes. *Iberorotalia reicheli* shows an
443 umbilicus composed of multiple funnels and piles distributed fairly regularly, quite
444 unlike the massive umbilical structure (some type of collumellar structure) that seems to
445 be present in the specimens of *Rotalia baetica* sp. nov. figured in the present paper.

446 **Genus *Rotorbinella* Bandy, 1944**

447 **Type species.** *Rotorbinella colliculus* Bandy, 1944.

448 ***Rotorbinella* sp.**

449 (Figure 13)

450 **Description.** The specimens are lenticular to low-conical shaped. The aperture is
451 simple. The chamber arrangement is low trochospiral with an evolute dorsal side and
452 involute ventral side. The umbilicus is filled with a single pile; the folia are short. The
453 dorsal surface is smooth. Proloculus of around 25 μm . The axial diameter is around 0.4–
454 0.5 mm, with 2.5–3 whorls; the height is about 0.2–0.3 mm.

455

456 **Rotaliids with uncertain affinities**

457 ? Subfamily **Rotaliinae** Ehrenberg, 1839

458 Genus *Suturina* Consorti, Vilallonga and Caus, 2017b

459 **Type species.** *Suturina globosa* Consorti, Vilallonga and Caus, 2017b.

460 **Remarks.** The genus *Suturina* was formerly defined by Consorti et al. (2017b) from the
461 Campanian of the Montsec Mountains (Pyrenees). The original diagnosis given is
462 complete but some structural elements cannot be properly observed in the material
463 figured. Notably, this is the case for the umbilical plate, the presence of which is not
464 clear in any of the specimens illustrated. Considering these limitations, we have
465 followed the description given in Consorti et al. (2017b, pg. 291) as a guide for the
466 generic identification of our specimens. There remains a need to conduct a study of
467 additional type material of the type species *S. globosa* Consorti et al., 2017b, focused on
468 the clarification and illustration of all its architectural features.

469 *Suturina minima* sp. nov.

470 (Figures 14–16, 17A–H)

471 LSID urn:lsid:zoobank.org:act:151F60CA-6511-457B-8DA1-FF09C7341968

472 **Etymology.** From the Latin word *minimus*, referring to its small size.

473 **Types.** The holotype is MGB 60335 LP02.036 (Fig. 14C). The other specimens
474 illustrated in Figures 14–16 are paratypes.

475 **Type horizon and locality.** Calizas de la Rambla de los Gavilanes Fm, upper
476 Campanian, *Penya del Romaní Hill* (Pinet, València, Spain).

477 **Diagnosis.** Lamellar-perforated test with coarsely perforated wall. Low-trochospiral
478 shell with rounded periphery. Simple aperture in an interiomarginal position. Dorsal
479 side evolute and flat with no ornamentation. Dorsal chamber sutures slightly marked.

480 Ventral side flat to slightly convex. Umbilical structure narrow and dominated by the
481 extension of the folia. Successive folia not fused, producing multiple and superposed
482 foliar chamberlets in the central part of the umbilical structure. Main lateral chamber
483 wall and folium wall separated by marked indentation or notch and by an umbilical-
484 plate suture. Main chamber lumen and spiral passage separated by an umbilical plate.
485 Peripheral cavities delimited by notch indentation and successive folia. Adult chambers
486 develop large folia, folded on the adaxial side. No dimorphism observed. Protoconch
487 diameter of around 24 μm and deutoconch of about 23 μm . Shell composed of around
488 2 whorls. Adult shells with a diameter of 260 to 380 μm and height of 140 to 210 μm ,
489 yielding a mean height-to-diameter ratio of about 0.54.

490 **Differential diagnosis.** *Suturina minima* sp. nov. differs from *S. globosa* from the
491 Campanian–lowermost Maastrichtian rocks in the Serres Marginals (Lleida, N Spain) in
492 having a smaller diameter, 0.3 mm vs. 0.8–1.2 mm, and smaller height, 0.2 mm vs.
493 0.5–0.7 mm, respectively. The proloculus is also smaller in the former than in the latter,
494 24 μm vs 40 μm . Although both morphotypes, *S. minima* sp. nov. and *S. globosa*, have
495 the same biostratigraphical distribution, we have considered them as two different
496 species because the vast majority of the specimens found in the Prebetic domain show a
497 relative homogeneity in terms of morphometry, being smaller than the type species.

498 **Remarks.** The specimens figured as *Stensioeina surrentina* Torre, 1967, by Luperto
499 Sinni (1976) from Murge, Italy, are very similar to *Suturina globosa* in terms of size
500 and shell architecture. More material is needed to carry out future architectural studies
501 of both morphotypes to confirm or to rule out whether they are the same species.

502 *Suturina globosa* Consorti, Vilallonga and Caus, 2017b

503 (Figure 17I–K)

504 1976 *Stensiöina surrentina* Torre; Luperto Sinni: tavola 53, figs. 1–5.

505 2017b *Suturina globosa* Consorti, Vilallonga and Caus; Consorti et al.: figs. 6.1–8, 10–
506 17.

507 2017b *Suturina* cf. *globosa* Consorti, Vilallonga and Caus; Consorti et al.: figs. 7.2–3.

508 **Description.** The material found is very scarce, but the specimens found seem to be
509 architecturally close to the type species of the genus *Suturina*. The shell has 2–3 whorls
510 and a diameter of around 0.8 mm. The chambers are rounded, increasing considerably in
511 size through the ontogeny. The dorsal side is flat and the sutures are marked. The
512 umbilicus is filled with non-fused folia.

513 **Other taxa excluded from the Rotalioidea according to Hottinger, 2014**

514 Subfamily **Pararotaliinae** Reiss, 1963

515 **Remarks.** According to Hottinger et al. (1991) and Hottinger (2014), the subfamily
516 Pararotaliinae includes taxa whose shell-architecture consists of a low trochospiral
517 chamber arrangement, evolute on the dorsal side and involute on the ventral side, simple
518 aperture, toothplates and canal-system composed of intraseptal and spiral-umbilical
519 canals. Some genera exhibit a simple enveloping canal system generated by the
520 covering of the interocular intraseptal space by the outer lamellae. Externally, the
521 specimens are characterized by being strongly ornamented, some of them possibly
522 having spines and keeled periphery. Despite the use of the term “enveloping canal
523 system” to describe some genera belonging to Pararotaliinae, it should be underlined
524 that this canal system is much simpler than that of other groups such as the calcarinids
525 or siderolitids (Hottinger and Leutenegger, 1980, Wannier, 1980), for which this term is
526 more commonly used. The enveloping canal system of these latter groups consists of

527 lateral meshes that differ in complexity with the canals being formed by the so-called
528 “flying covers” in Pararotaliinae (see Figs. 3 and 4 in Hottinger, 1991). In order to avoid
529 any possible misinterpretation, the term “enveloping canal system” should always be
530 accompanied by a clarification of the diagnostic criteria on which the identification is
531 based.

532 **Genus *Neorotalia* Bermúdez, 1952**

533 **Type species.** *Rotalia mexicana* Nuttall, 1928 accepted as *Neorotalia burdigalensis*
534 (d'Orbigny, 1852).

535 **Remarks.** The canals of the so-called “enveloping canal system” observed in the
536 specimens of the genus *Neorotalia* is the main architectural difference from the genus
537 *Pararotalia* Le Calvez, 1949.

538 ***Neorotalia? pinetensis* sp. nov.**

539 (Figures 18, 19)

540 LSID urn:lsid:zoobank.org:act:EB4C7246-C587-4EB4-BD69-FA56D4FD8E68

541 **Etymology.** From the type locality of Pinet.

542 **Types.** The holotype is MGB 60316 LP04.005 (Fig. 18B). The other specimens
543 illustrated in Figure 18 are paratypes.

544 **Type horizon and locality.** Calizas de la Rambla de los Gavilanes Fm, upper
545 Campanian, *Penya del Romaní Hill* (Pinet, València, Spain).

546 **Diagnosis.** Lamellar-perforated test with trochospiral chamber arrangement and keeled
547 periphery. Dorsal side planoconvex, evolute and ornamented with beads. Ventral side
548 convex and involute. Simple aperture consisting of a narrow slit in an interiomarginal
549 position. Umbilicus composed of a thick, dense structure composed of pile with

550 furrows. Chamber lumen shows a “toothplate” producing a primary spiral canal. Simple
551 enveloping canal system formed by outer lamellae covering the interocular intraseptal
552 spaces seems to be present (see Fig. 18.A). The shells are between 0.5 to 0.7 mm in
553 diameter and about 0.3 to 0.4 mm in height (thickness) with three and a half whorls.
554 Embryo very small, formed by a protoconch and a deutoconch. Protoconch of around
555 18 μm ; deutoconch of about 22 μm . No dimorphism has been observed.

556 **Remarks.** We have left our morphotype in open nomenclature at generic level because
557 of the complexity in identifying from thin-section the flying covers, which are the main
558 diagnostic criterion that differentiates *Neorotalia* from *Pararotalia*.

559 **Differences and similarities.** The Mesozoic new species *N.? pinetensis* (maximum
560 diameter 0.7 mm) is smaller than the Cenozoic species *N. burdigalensis* (d’Orbigny,
561 1852), *N. mexicana* (Nutall 1952) (maximum diameter 1.1 mm) (synonym of *N.*
562 *burdigalensis* according to Poignant, 1998), *Neorotalia lithamnica* (Uhlig, 1886)
563 (maximum diameter around 1 mm) (synonym of *N. burdigalensis* according to Poignant
564 and Pujol, 1978), *Neorotalia omanensis* Al-Sayigh, 2013 (maximum diameter 2.3 mm),
565 *Neorotalia viennoti* (Greig, 1935) (maximum diameter around 2 mm), *Neorotalia*
566 *calcar* (d’Orbigny in Deshayes, 1830) (maximum diameter around 1.5 mm), and
567 *Neorotalia gaimardi* (d’Orbigny in Fornasini, 1908) (maximum diameter around 1 mm).

568 In terms of size and external morphology, the species *Neorotalia? pinetensis* sp. nov.
569 seems to be closely related to the group of neorotalias from the Eocene of Alicante. The
570 diameter of its test is similar to *Neorotalia alicantina* Colom, 1954, being around 0.7
571 mm; however, the latter has a biconvex test. *Neorotalia bicarinata* Colom, 1954, is
572 similar to *N.? pinetensis* sp. nov. in having a dissymmetric test, but the former is smaller
573 (around 0.4 mm in diameter) and also lacks the ventral keel. *Neorotalia minuta* Colom,

574 1954, is similar to *N.? pinetensis* sp. nov. in having a keeled periphery, but the former is
575 smaller (around 0.4 mm in diameter) and has a biconvex test. The neorotalias described
576 from the Oligocene of Mallorca, *N. ornatissima* Escandell and Colom, 1962, and *N.*
577 *semiornata* Escandell and Colom, 1962, are also different from *N.? pinetensis* sp. nov.
578 The tests of *N. semiornata* are smooth, biconvex and larger (diameter of around 1–2
579 mm) than those of the latter. The tests of *N. ornatissima* are biconvex and larger
580 (diameter of around 2 mm) than those of the new species. A study of the internal
581 structure of topotypes of these and other species of *Neorotalia*, described only based on
582 their external features, should be carried out in future in order to define the inner
583 skeletal elements, this being essential to obtain a reliable classification, as in all LBF.
584 The species *Neorotalia tethyana* Boudagher-Fadel and Price, 2013, is a rotaliform
585 species from the upper Oligocene–earliest Miocene of Java that calls for a restudy, as its
586 internal structure is not clear from observing the scarce specimens figured. In any case,
587 its maximum diameter, of 1.5 mm, is larger than that of *N.? pinetensis* sp. nov.
588 The species *Neorotalia? pinetensis* sp. nov. is architecturally close to *Neorotalia?*
589 *cretacea* Consorti et al., 2017a, from the lower Campanian of the Lepini Mountains,
590 differing mainly in the smaller size and in the flatter dorsal side of the former.
591 Nonetheless, in our opinion, no toothplates are visible in the specimens figured in
592 Consorti et al. (2017a, see Fig. 11 of this paper).

593

594 Genus *Pararotalia* Le Calvez, 1949

595 **Type species.** *Rotalina inermis* Terquem, 1882.

596 *Pararotalia tuberculifera* (Reuss, 1862)

597 (Figure 20)

598 1862 *Rotalia tuberculifera* Reuss: p. 313, pl. 2, fig. 2.
599 1959 *Pararotalia tuberculifera* (Reuss); Hofker: p. 345, fig. 132–134.
600 1966 *Pararotalia tuberculifera* (Reuss); Hottinger: fig. 9b, p. 296.
601 2007 *Pararotalia tuberculifera* (Reuss); Boix: pl. XXIII and XXIV.
602 2009 *Pararotalia tuberculifera* (Reuss); Boix et al.: Figs. 12.1–12.21.

603 **Description.** The shell is lamellar-perforated, biconvex to planoconvex, and low-
604 trochospiral chamber arrangement. The periphery is keeled. The ventral side shows a
605 central plug. The dorsal side presents ornamentation based on beads. The proloculus is
606 small, around 12 μm in diameter, with a maximum diameter of around 0.4 mm.

607

608 **5. Biostratigraphy based on larger benthic foraminifera**

609 **5.1. Larger rotaliid assemblages**

610 The study of the larger foraminifera found in the samples collected has allowed the
611 identification of two assemblages:

612 **Assemblage 1.** This assemblage is characterized by the presence of the rotaliids
613 *Neorotalia? pinetensis* sp. nov., *Rotalia baetica* sp. nov., *Suturina globosa*, *S. minima*,
614 and *Rotalispira scarsellai*. They are found in association with other foraminifera, such
615 as *Goupillaudina shirazensis* Rahaghi, *Praestorsella roestae* (Visser), *Pararotalia*
616 *tuberculifera*, *Praesiderolites douvillei* Wannier, *Orbitoides* cf. *media* (d'Archiac),
617 indeterminate Gavelinellidae, small agglutinated and simple miliolids and discorbids.

618 In the Peña del Román section, other species found include *Nummofallotia cretacea*
619 (Schlumberger), *Haddonina* sp., *Cuneolina cylindrica* Henson, *Navarella joaquinii* Ciry

620 & Rat, *Stomatorbina binkhorsti* (Reuss), aff. *Sivasella* sp., *Sirtina ornata* (Rahaghi),
621 *Lepidorbitoides* cf. *campaniensis* van Gorsel, “*Orbitoides*” cf. *concevatus* Rahaghi, *O.*
622 *megaliformis* Papp & Küpper, *Pseudosiderolites vidali* (Douvillé), and cf. *Wannierina*
623 sp. (Fig. 21).

624 In the Serra de les Agulles section, other foraminifera have been identified including
625 *Moncharmontia* sp., *Dictyopsella* sp., *Idalina antiqua* Schlumberger and Munier-
626 Chalmas, *Murgeina apula* (Luperto Sinni), *Lepidorbitoides* sp., *Orbitoides* sp. and
627 *Arnaudiella grossouvrei* Douvillé (Fig. 22).

628 At the bottom of the Serra Grossa section, the other species found are *Dictyopsella* sp.,
629 *Nezzazzatinella* sp., *Fleuryana* sp., *Scandonea* sp., *Cuvillerinella* cf. *salentina* Papetti
630 and Tedeschi, *Rotorbinella* sp., and *Pseudosiderolites vidali*. At the top of this section,
631 the following species were identified: *Nezzazzatinella* sp., *Fleuryana* sp., *Cuneolina*
632 *cylindrica*, *Murgeina apula*, *Murciella* aff. *cuvillieri* Fourcade, *Orbitoides* cf.
633 *megaliformis*, *Lepidorbitoides* cf. *bisambergensis* and *Siderolites* cf. *praecalciatrapoides*
634 Neumann (Fig. 23).

635 **Biostratigraphical discussion.** The biostratigraphic distribution of *Rotalispira*
636 *scarsellai* has been reported classically from Coniacian to Campanian deposits, but in
637 Frijia et al. (2015) the first occurrence of this species was constrained to upper
638 Turonian. Consorti et al. (2017a) constrained its age to upper Santonian?–lower
639 Campanian deposits in the Lepini Mountains (Central Italy) and middle Campanian in
640 southern Italy. *Suturina globosa* were also reported by Consorti et al. (2017b) in the
641 lower?–middle Campanian deposits in the southern Pyrenees (Spain). *Praesiderolites*
642 *douvillei*, *Arnaudiella grossouvrei* and *Pseudosiderolites vidali* were reported in the
643 middle–upper Campanian in the southern Pyrenees (Wannier, 1983; Robles-Salcedo,

644 2014). Schlüter et al. (2008) dated the deposits in the type locality of *Cuvillierinella*
645 *salentina* as late Campanian. The species *Siderolites praecalcitrapoides* and *Orbitoides*
646 *cf. megaliformis* were reported in the deposits of the uppermost Campanian in the
647 southern Pyrenees (Caus et al., 1996, 2016; Robles-Salcedo et al., 2018). The
648 representatives of the genus *Murciella* Fourcade and other similar forms was limited
649 from upper Campanian to lower Maastrichtian deposits in several studies along the
650 Tethyan realm (see Fourcade, 1966; De Castro, 1988; Ramírez del Pozo and Martín-
651 Chivelet, 1994; Vicedo, 2009, Fleury, 2018, among others).

652 According to this information obtained from the literature, the rotaliid assemblage 1 of
653 the Prebetic would be dated as middle to late Campanian, given that no Maastrichtian
654 fauna have been identified. On the other hand, it is important to note that the
655 assemblage of the uppermost interval in the Serra Grossa section, which presents
656 several taxa in open nomenclature (Fig. 3), might include the Campanian/Maastrichtian
657 boundary. Further studies of the murciellas, among other taxa found, would likely help
658 constrain the Campanian–Maastrichtian boundary.

659 **Assemblage 2.** This assemblage is characterized by *Suturina minima* sp. nov.,
660 *Plumopraeolockhartia solanensis* sp. nov. and *Pseudosulcoperculina bocairentina* gen.
661 et sp. nov. In the Serra de la Solana section they are found in association with *Idalina*
662 *antiqua* Schlumberger & Munier-Chalmas, *Nummofallotia cretacea* (Schlumberger),
663 *Cibicides* sp., *Goupillaudina* sp., *Praestorsella roestae*, *Selimina spinalis* Inan,
664 *Fissolphidium operculiferum* Smout, *Sirtina orbitoidiformis* Brönnimann and Wirz,
665 *Sivasella monolateralis* Sirel and Gündüz 1978, *Hellenocyclina beotica* Reichel,
666 *Omphalocyclus macroporus* (Lamarck), *Orbitoides apiculata* Schlumberger, *Siderolites*
667 *calcitrapoides* Lamarck, small agglutinated, simple miliolids and discorbids (Fig. 24).

668 **Biostratigraphical discussion.** This assemblage gives an age of late Maastrichtian,
669 which is in accordance with dates proposed in the studies of Pons et al. (1994) and
670 Granero et al. (2018). These deposits of the interval studied represent the latest deposits
671 of the Cretaceous period in the area.

672 **5.2. Correlation with other sectors of the Prebetic**

673 The deposits containing these LBF assemblages can be correlated at a regional scale
674 with the three units defined in terms of sequential stratigraphy for the Coniacian–
675 Maastrichtian from the Prebetic domain (Ramírez del Pozo and Martín-Chivelet, 1994;
676 Martín-Chivelet and Chacón, 2007). These authors described three megasequences or
677 “event bounded stratigraphic units (EBUSs)” separated by major discontinuities. The
678 first and oldest unit was dated as Coniacian–lowermost Campanian by Ramírez del Pozo
679 and Martín-Chivelet (1994), , age that was updated as upper Coniacian to upper
680 Santonian by Martín-Chivelet and Chacón (2007), being lithostratigraphically
681 represented by the Margas de Alarcón and Calizas y brechas calcáreas de Sierra de Utiel
682 Fms. The second as lower Campanian–lower Maastrichtian by Ramírez del Pozo and
683 Martín-Chivelet (1994) , and uppermost Santonian–lower Maastrichtian by Martín-
684 Chivelet and Chacón (2007), corresponding to the Calizas del Carche and Calizas de la
685 Rambla de los Gavilanes Fms. And the third and youngest unit as late Maastrichtian in
686 age with the Margas de los Cerrillares, Calizas Arenosas del Molar and Margas de
687 Raspay Fms. According to Ramírez del Pozo and Martín-Chivelet (1994) and Martín-
688 Chivelet and Chacón (2007) the ages given for the megasequences were supported by
689 correlations with equivalent units containing planktonic foraminifera. These authors
690 distinguished the planktonic zones for the latter two EBSUs or megasequences, from the
691 bottom to the top:

- 692 - Second megasequence or EBSU-2: *Dicarinella asymetrica* (only its uppermost
693 part), *Globotruncanita elevata*, *Globotruncana ventricosa*, *Rodotruncana*
694 *calcarata*, *Globotruncana falsostuarti* and *Gansserina gansseri* Zones (only its
695 lower-middle part).
- 696 - Third megasequence or EBSU-3: upper part of the *G. gansseri* Zone and
697 *Abathomphalus mayaroensis* Zone.

698 Nevertheless, this work propose to recalibrate these chronostratigraphical ages based on
699 the biozone of the planktonic foraminifera in Gradstein et al. (2012), suggesting that the
700 second megasequence ranges from late Santonian to late Campanian and the third from
701 early to late Maastrichtian.

702 Regarding LBF, in the case of the second megasequence, Ramírez del Pozo and Martín-
703 Chivelet (1994) identified the biozone of the *Murciella cuvillieri* Fourcade (in the
704 present study, *Murciella* aff. *cuvillieri*) and other rhapsydioninid relatives, found in this
705 study in the same unit as the rotaliids *Neorotalia? pinetensis* sp. nov., *Rotalia baetica*
706 sp. nov., *Suturina minima* sp. nov., *Suturina globosa*, *Rotalispira scarsellai* and
707 *Rotorbinella* sp. Those authors dated this megasequence by correlation with the
708 *Globotruncanita elevata*, *Globotruncana ventricosa*, *Radotruncana calcarata*, and
709 *Globotruncana falsostuarti* zones and the lowermost *Gansserina gansseri* zone. In the
710 case of the younger and third megasequence, Ramírez del Pozo and Martín-Chivelet
711 (1994) cited the species *Sulcoperculina dickersoni* var. *vermunti* (Thiadens), specimens
712 of which we have identified as *Pseudosulcoperculina bocairentina* gen. et sp. nov.,
713 together with *Plumopraelockhartia solanensis* sp. nov. and *Suturina minima* sp. nov., in
714 the biozone of *Siderolites calcitrapoides* Lamarck and ascribed to the *Gansserina*
715 *gansseri* zone.

716 In the case of the Prebetic areas studied in the present paper, the deposits containing
717 assemblage 1 can be correlated with the second megasequence or EBSU-2 from middle
718 to late Campanian ages, and assemblage 2 with the third from late Maastrichtian ages,
719 extending the geographical distribution of the LBF biozones identified from the
720 Murcian sector to the Valencia and Albacete Prebetic sector.

721

722 **6. Paleobiogeographic and phylogenetic discussion**

723 **6.1. The occurrence of *Sulcoperculina*-like morphotypes in both sides of the Late** 724 **Cretaceous Atlantic**

725 The genus *Sulcoperculina* was erected by Thalmann in 1939 to accommodate the
726 species *Camerina dickersoni* Palmer, 1934 (type species of the genus), *C. cubensis*
727 Palmer, 1934 and *C. vermunti* Thiadens, 1937 from the Upper Cretaceous of Cuba.
728 Since then, several species have been described and also assigned to the genus
729 *Sulcoperculina*, namely, *S. cosdeni* Applin and Jordan, 1945, *S. globosa* Cizancourt,
730 1949, *S. obesa* Cizancourt, 1949, *S. angulata* Brown and Bronnimann, 1957, *S. minima*
731 Seiglie and Ayala-Castañares, 1963, *S. diazi* Seiglie and Ayala-Castañares, 1963, *S.*
732 *inaequalis* Ho, 1976 and *S. kugleri* Hottinger, 1977. All the species seem to have
733 common features, such as the marginal sulcus and the involute spiral chamber
734 arrangement. Nevertheless, among the species assigned to *Sulcoperculina*, there are
735 significant differences that deserve to be discussed. According to the detailed study of
736 Cole (1947) and other observations by previous authors (e.g., Voorwijk, 1937;
737 Vaughan, 1945), remarkable variability in terms of morphology and size can be
738 observed in closely related *Sulcoperculina* populations. These observations led Cole
739 (1947) to consider some of the species described until then as infraspecific varieties (see

740 pg. 235 in Cole, 1947), ruling out that they constituted distinct natural species. Leaving
741 aside this hypothesis and other synonymies proposed by various authors (see also Frost,
742 1974), observing in broad terms the morphology of the specimens figured in the
743 literature to date, it seems that there are at least two different morphotypes of
744 sulcoperculinas. On the one hand, there is one large morphological group represented by
745 the type species, *S. gr. dickersoni*, which have a nearly bilateral symmetry and
746 ornamentation restricted to the central plug and inflated septal sutures or beads. Its shell
747 has an extremely low to almost planispiral chamber arrangement. Apart from the type,
748 the vast majority of the species described, namely, *S. vermunti*, *S. cubensis*, *S. cosdeni*,
749 *S. globosa*, *S. obesa*, *S. angulata*, *S. minima* and *S. diazi* seem to have similar
750 architecture and, therefore, they would be included in the same group. On the other
751 hand, there is a second morphotype represented by Hottinger's species, *S. kugleri*,
752 which is characterized by a clear trochospiral chamber arrangement, asymmetric shell
753 and marked feathered ornamentation on the ventral chamber wall. Our observations
754 regarding the separation of the American forms into two groups based on their
755 dissimilar test-architecture are in accordance with those of Hottinger (1977) who stated
756 that the Campanian trochospiral species *S. kugleri* should be separated from the
757 Maastrichtian planispiral forms (see pg. 29 in Hottinger, 1977). The species *S.*
758 *inaequalis* from the Upper Cretaceous of Tibet, China, could belong to *S. gr. kugleri*
759 according to its assymetrical shell. Nonetheless, the generic ascription of the species *S.*
760 *inaequalis* should be revised in future as it appears to show some differences in its
761 marginal and umbilical structures.

762 The resemblance of *P. bocairentina* gen. et sp. nov. to the trochospiral species *S. kugleri*
763 Hottinger, 1977, from the Campanian of Jamaica prompts discussion about the origin of
764 their architectural similarities. According to Hottinger (1977), the trochospiral structure

765 of *S. kugleri* found in Jamaica can be considered “primitive” with respect to the other
766 species of sulcoperculinas with planispiral coiling, which develop later during the
767 Maastrichtian ages in the American-Caribbean domain. The presence of the trochospiral
768 growth in architecturally similar younger forms, in particular in the Maastrichtian
769 “sulcoperculina-like” specimens from the western Tethys, raises the question of
770 dispersal versus vicariance groups. This would mean either the persistence of that
771 primitive rotaloid architecture between older and younger phylogenetically related
772 forms or an environmental adaptation in species of different phylogenetic lines, not
773 directly related, represented by *S. kugleri* for the American forms and *P. bocairentina*
774 gen. et sp. nov. for the Tethyan forms.

775 The relationship between the *Pseudosulcoperculina?* sp. from the early Maastrichtian of
776 the Atlantic Pyrenean domain and *P. bocairentina* gen. et sp. nov. from the lowermost
777 upper Maastrichtian of the western Tethys also deserves careful analysis in the future.
778 Further, these forms should be compared with other rotaliiforms which are cited as
779 *Sulcoperculina*, but poorly illustrated and difficult to identify, in other palaeogeographic
780 areas of the Tethyan domain (Butterlin, 1967, Luperto Sinni and Ricchetti, 1978,
781 Abdelghany, 2003; Dimitrova, 2003; Al-Dulaimi and Al-Obaidy, 2017; Akmaluddin et
782 al., 2019, among others). The possibly existence of a paleo-Gulf-stream during the late
783 Cretaceous connecting the American and the Tethyan domains (Fourcade and Michaud,
784 1987) would be in favor of considering the dispersion of species as key to find closely
785 related forms in both sides of the Atlantic. Nonetheless, the answer to all these
786 questions is far beyond the scope of the present paper. Reaching firm conclusions in
787 terms of phylogenetic relationships would need a reanalysis of all the morphotypes
788 found so far in the American, Pyrenean and Tethyan domains, and with a solid
789 stratigraphical framework.

790 In any case, the trochospiral *Sulcoperculina*-like forms of both sides of the Atlantic
791 ocean show architectural differences, but also similarities, which are proven in the
792 present study. Considering all the information available to date, it seems that the
793 operculiniform planispiral symmetrical younger forms from the American-Caribbean
794 domain, *S. gr. dickersoni*, are absent in the eastern domains, Pyrenean and Tethyan
795 domains, only the similar trochospiral rotaloid forms having spread widely. The future
796 revision of the entire group would not only lead to a better understanding of the
797 evolutionary trends and the phylogenetic relationships of the species involved, but also
798 to a redefinition of the architectural traits of the genus *Sulcoperculina*, which should be
799 considered to date as an endemic form of the American-Caribbean palaeobioprovince.

800 **6.2. Early evolution of praelockhartiines**

801 The cavities observed in the umbilical structure of *Plumopraelockhartia solanensis* gen.
802 et sp. nov. makes this species resemble to the representatives of the subfamily
803 Praelockhartiinae Vicedo and Robles-Salcedo, 2019, defined in the early Paleocene of
804 the Oman Mountains. The ascription of that species to this subfamily roots the origin of
805 the group of lokhartiines sensu lato, which would include the closely related forms
806 belonging to both, Praelockhartiinae and Lockhartiinae, back to the Upper Cretaceous
807 and expands its palaeogeographic distribution to the westernmost Tethys.

808

809 **7. Conclusions**

810 The revision of the larger rotaliid specimens found in the Upper Cretaceous series from
811 the Valencian sector of the external Prebetic domain has allowed us to present the
812 following:

- 813 1. Five new species and two new genera, namely, *Pseudosulcoperculina*
814 *bocairentina* gen. et sp. nov., *Plumopraelockhartia solanensis* gen. et sp. nov.,
815 *Rotalia baetica* sp. nov., *Suturina minima* sp. nov., and *Neorotalia? pinetensis*
816 sp. nov.
- 817 2. The rothaliids found characterize two different assemblages. The older
818 assemblage is composed of *Neorotalia? pinetensis* sp. nov., *Rotalia baetica* sp.
819 nov., *Suturina globosa*, *Rotorbinella* sp., *Pararotalia tuberculifera* and
820 *Rotalispira scarsellai* that were found in middle to upper Campanian deposits.
821 The younger assemblage is composed of *Pseudosulcoperculina bocairentina*
822 gen. et sp. nov., *Plumopraelockhartia solanensis* gen. et sp. nov. and
823 *Pararotalia tuberculifera* that were found in upper Maastrichtian deposits. The
824 species *Suturina minima* sp. nov. was found in both assemblages, dated in
825 deposits from middle Campanian to Maastrichtian.
- 826 3. The rothaliid assemblages can be correlated with the main megasequences
827 defined for the Prebetic, extending the geographical distribution of the LBF
828 biozones and enhancing their regional biostratigraphical value.
- 829 4. A discussion based on a detailed comparison of the test architecture of the
830 species found with other similar taxa from the Caribbean, Pyrenean and Tethyan
831 domains reveals significant differences, but also similarities, among the
832 *Sulcoperculina*-like forms. According to all the data available up to now, the
833 genus *Sulcoperculina* would be restricted to the American-Caribbean
834 palaeobioprovince and, therefore, its use in the species ascription of other realms
835 should be avoided.
- 836 5. A proposal to root the origin of lockhartiines sensu lato back to the late
837 Cretaceous.

838

839 ACKNOWLEDGMENTS

840 Financial support for the present study was received within the framework of the
841 research and collections projects of the Museu de Ciències Naturals de Barcelona
842 (MCNB). Many thanks are due to Dr Miguel Navas and Emma Asensio, technicians of
843 the Documentation Centre of the museum, for supplying references, and to preparator
844 Dr Gerard Lucena of the Geology and Palaeontology MCNB Lab, for his work in
845 producing the excellent thin sections of carbonate rocks. We also acknowledge Dr.
846 Lorenzo Consorti and Prof. Esmeralda Caus for their valuable revision of the
847 manuscript. This research is a contribution to the project IBERINSULA (PID2020-
848 113912GB-100) from the Spanish Ministerio de Ciencia e Innovación (MICINN) and
849 the European Regional Development Fund (ERDF).

850

851 **References**

852 Abdelghany, O., 2003. Late Campanian–Maastrichtian foraminifera from the
853 Simsima Formation on the western side of the Northern Oman Mountains.
854 Cretaceous Research 24, 391–405. doi: 10.1016/S0195-6671(03)00051-X.
855 Akmaluddin, A., Virgiawan Agustin, M., Husein, S., Novian, M. I., Setiawan, N.
856 I., Barianto, D. H., Tampubolon, B. T., Eka Sapura, S., 2019. Late Cretaceous
857 sedimentary rock in Barito Basin, Indonesia: lithology, paleontology, and
858 paleoenvironment. Scientific Contributions Oil and Gas 42, 131–143. doi:
859 10.29017/SCOG.

860 Al-Dulaimi, S. I., Al-Obaidy, R. A., 2017. Biostratigraphy of Bekhme Formation
861 (Upper Cretaceous) in selected sections, Kurdistan region, northeast Iraq.
862 Iraqi Bulletin of Geology and Mining 13, 1–14.

863 Al-Sayigh, A. R. S., 2013. *Neorotalia omanensis* and *Operculina musawaensis*
864 from the Sultanate of Oman. Science and Technology 18, 41–53. doi:
865 10.24200/squjs.vol18iss0pp41-53.

866 Albrich, S., Frijia, G., Parente, M., Caus, E., 2014. The evolution of the earliest
867 representatives of the genus *Orbitoides*: Implications for Upper Cretaceous
868 biostratigraphy. Cretaceous Research 51, 22–34. doi:
869 10.1016/j.cretres.2014.04.013.

870 Albrich, S., Boix, C., Caus, E., 2015. Selected agglutinated larger foraminifera
871 from the Font de les Bagasses unit (early Campanian, southern Pyrenees).
872 Carnets de géologie (Notebooks on geology) 15, 245–267. doi:
873 10.4267/2042/57953.

874 Applin, E. R., Jordan, L., 1945. Diagnostic foraminifera from subsurface
875 formations in Florida. Journal of Paleontology 19, 129–148.

876 Arriaga, M. E., 2016. Patrones de Supervivencia y Recuperación de Los
877 Macroforaminíferos después de la Extinción en Masa del límite
878 Cenomaniense–Turonense. Universitat Autònoma de Barcelona, Barcelona,
879 149 pp.

880 Azañón, J. M., Galindo-Zaldívar, J., García-Dueñas, V., Jabaloy, A., 2002. Alpine
881 tectonics II: Betic Cordillera and Balearic Islands. In: The Geology of Spain.
882 The Geological Society of London, London, 401–416. doi: 10.1144/gospp.16.

883 Azema, J., Foucault, A., Fourcade, E., García-Hernández, M., González-Donoso, J.
884 M., Linares, A., Linares, D., López-Garrido, A. C., Rivas, P., Vera, J. A.,

885 1979. La Microfacies Del Jurásico y Del Cretácico de La Zonas Externas de
886 Las Cordilleras Béticas. Universidad de Granada, Granada. 86p., 46 lám. pp.

887 Bignot, G., 1972. Recherches Stratigraphiques Sur Les Calcaires Du Cretace
888 Superieur et de l'Eocene d'Istrie et Des Regions Voisien. Essai de Revision
889 Du Liburnien. Universite de Paris-5^o, Paris U.E.R. 63 sciences de la terre, 345
890 pp.

891 Boix, C., 2007. Foraminíferos Rotálids Del Cretácico Superior de La Cuenca
892 Pirenaica. Univertitat Autònoma de Barcelona, Barcelona, 139 pp.

893 Boix, C., Villalonga, R., Caus, E., Hottinger, L., 2009. Late Cretaceous rotaliids
894 (Foraminiferida) from the Western Tethys. Neues Jahrbuch für Geologie und
895 Paläontologie - Abhandlungen 253, 197–227. doi: 10.1127/0077-
896 7749/2009/0253-0197.

897 Boix, C., Frijia, G., Vicedo, V., Bernaus, J. M., Di Lucia, M., Parente, M., Caus,
898 E., 2011. Larger foraminifera distribution and strontium isotope stratigraphy
899 of the La Cova limestones (Coniacian–Santonian, ‘Serra del Montsec’,
900 Pyrenees, NE Spain). Cretaceous Research 32, 806–822. doi:
901 10.1016/j.cretres.2011.05.009.

902 Boudagher-Fadel, M. K., Price, G. D., 2013. The phylogenetic and
903 palaeogeographic evolution of the miogypsinid larger benthic foraminifera.
904 Journal of the Geological Society 170, 185–208. doi: 10.1144/jgs2011-149.

905 Brown, N. K., Brönnimann, P., 1957. Some Upper Cretaceous Rotaliids from the
906 Caribbean Region. Micropaleontology 3, 29–38.

907 Butterlin, J., 1967. Au sujet de la présence en Europe du genre *Sulcoperculina*
908 Thalmann, 1939. Revue de Micropaléontologie 10 (1), 61–64.

909 Caus, E., Gómez-Garrido, A., Simó, A., Sofiano, K., 1993. Cenomanian–Turonian
910 platform to basin integrated stratigraphy in the South Pyrenees (Spain).
911 Cretaceous Research 14, 531–551.

912 Caus, E., Bernaus, J. M., Gomez-Garrido, A., 1996. Biostratigraphic utility of
913 species of the genus *Orbitoides*. The Journal of Foraminiferal Research 26,
914 124–136.

915 Caus, E., Teixell, A., Bernaus, J. M., 1997. Depositional model of a Cenomanian–
916 Turonian extensional basin (Sopeira Basin, NE Spain): Interplay between
917 tectonics, eustasy and biological productivity. Palaeogeography,
918 Palaeoclimatology, Palaeoecology 129, 23–36. doi: 10.1016/S0031-
919 0182(96)00051-X.

920 Caus, E., Frijia, G., Parente, M., Robles-Salcedo, R., Villalonga, R., 2016.
921 Constraining the age of the last marine sediments in the late Cretaceous of
922 central south Pyrenees (NE Spain): Insights from larger benthic foraminifera
923 and strontium isotope stratigraphy. Cretaceous Research 57, 402–413. doi:
924 10.1016/j.cretres.2015.05.012.

925 Chiocchini, M., Farinacci, A., Mancinelli, A., Molinari, V., Potetti, M., 1994.
926 Biostratigrafia a foraminiferi, dasicladali e calpionelle delle successioni
927 carbonatiche mesozoiche dell’Appennino centrale (Italia). In: Mancinelli, A.
928 (ed.) Biostratigrafia Dell’Italia Centrale. Studi Geologici Camerti, Volume
929 Speciale. 9–129.

930 Chiocchini, M., Chiocchini, R.A., Didaskalou, P., Potetti, M., 2008.
931 Microbiostratigrafia del Triassico superior, Giurassico e Cretacico in facies di
932 piattaforma carbonatica del Lazio centro-meridionale e Abruzzo: revision

933 finale, in: Chiocchini, M. (Ed.), Memorie Descrittive Della Carta Geologica
934 d' Italia. Torino, pp. 84, 5–170.

935 Chiocchini, M., Pampaloni, M.L., Pichezzi, R.M., 2012. Microfacies and
936 microfossils of the Mesozoic carbonate successions of Latium and Abruzzi
937 (Central Italy). Memorie per Servire alla Descrizione della Carta Geologica
938 D'Italia. Memorie per Servire alla Descrizione della Carta Geologica D'Italia,
939 ISPRA, Dipartimento Difesa del Suolo. 17.

940 Cizancourt, M. de., 1949. Matériaux pour la paléontologie et la Stratigraphie des
941 régions Caraïbes. Bulletin de la Société géologique de France 5, 663–674.

942 Cole, W. S., 1947. Internal structure of some floridian foraminifera. Bulletins of
943 American Paleontology 31, 227–245, pl. 21.

944 Colom, G., 1954. Estudio de las biozonas con foraminíferos del Terciario de
945 Alicante. Boletín del Instituto Geológico y Minero de España 66, 101–451.

946 Consorti, L., Rashidi, K., 2018. A new evidence of passing the Maastrichtian–
947 Paleocene boundary by larger benthic foraminifers: The case of *Elazigina*
948 from the Maastrichtian Tarbur Formation of Iran. Acta Palaeontologica
949 Polonica 63, 595–605. doi: 10.4202/app.00487.2018.

950 Consorti, L., Caus, E., Frijia, G., Yazdi-Moghadam, M., 2015. *Praetaberina* new
951 genus (type species: *Taberina bingistani* Henson, 1948): a stratigraphic
952 marker for the late Cenomanian. Journal of Foraminiferal Research 45, 378–
953 389.

954 Consorti, L., Villalonga, R., Caus, E., 2017a. New rotaliids (Benthic Foraminifera)
955 from the late cretaceous of the Pyrenees in Northeastern Spain. Journal of
956 Foraminiferal Research 47, 284–293. doi: 10.2113/gsjfr.47.3.284.

957 Consorti, L., Frijia, G., Caus, E., 2017b. Rotaloidean foraminifera from the Upper
958 Cretaceous carbonates of Central and Southern Italy and their
959 chronostratigraphic age. *Cretaceous Research* 70, 226–243. doi:
960 10.1016/j.cretres.2016.11.004.

961 De Castro, P., 1988. Les Alveolinides du Cretace d'Italie. *Benthos '86* 2, 401–416.

962 Deshayes, G. P., 1830. Encyclopédie méthodique ou par ordre de matières.
963 Histoire naturelle des Vers et Mollusques. Encyclopédie Méthodique 2, 1–
964 256.

965 Dimitrova, E., 2003. First data about the presence of genera *Planorbulina* and
966 *Sulcoperculina* in the Upper Cretaceous and Paleogene in Bulgaria. Review of
967 the Bulgarian Geological Society 64, 55–57.

968 Drooger, C. W., 1960. Some early rotaliid Foraminifera. II. Proceedings of the
969 Koninklijke Nederlandse Akademie van Wetenschappen, Amsterdam, ser. B,
970 63, 302–318.

971 Eckstaller, W., 1993. Geologische Kartierung Der Küstencordilliere Zwischen
972 Alcira Und Tabernes de La Valldigna (Prov. Valencia/ SE Spanien).
973 Universität München 85, Tafeln 13 pp.

974 Escandell, B., Colom, G., 1962. Una revisión del Nummulítico mallorquin. *Notas y*
975 *Comunicaciones del Instituto Geológico y Minero de España* 66, 73–142.

976 Finlay, H., 1939. New Zealand Foraminifera; key species in stratigraphy-No 1.
977 *Trans. R. Soc. New Zeal.* 1, 504–532.

978 Fleury, J.J., 2018. Rhapydioninidés du Campanien-Maastrichtien en région
979 méditerranéenne: Les genres *Murciella*, *Sigalveolina* n. gen. et
980 *Cyclopseudomia*. *Carnets Geologie* 18 (11), 233–280.

981 Fornasini, C., 1908. Illustrazione di specie orbignyane di Nodosaridi, di Rotalidi e
982 d'altri foraminiferi. Memorie della Reale Accademie della Scienze
983 dell'Istituto di Bologna, Scienze Naturali 6, 41–54.

984 Fourcade, E., 1966. Murciella cuvillieri n. gen. n. sp. nouveau foraminifère du
985 Sénonien supérieur du sud-est de l'Espagne. Revue de Micropaléontologie 9,
986 147–155.

987 Fourcade, E., 1970. Le Jurassique et Le Cretacé Aux Confins Des Chaînes
988 Bétiqes et Ibériques (Sud-Est de l'Espagne). Université de Paris, Paris, 437
989 pp.

990 Fourcade, E., Michaud, F., 1987. L'ouverture de l'Atlantique et son influence sur
991 les peuplements des grands foraminifères des plates-formes péri-océaniques
992 au Mésozoïque. Geodinamica Acta 1 (4/5), 247–262.

993 Frijia, G., Parente, M., Lucia, M. Di, Mutti, M., 2015. Carbon and Strontium
994 isotope stratigraphy of the Upper Cretaceous (Cenomanian–Campanian)
995 shallow-water carbonates of southern Italy: chronostratigraphic calibration of
996 larger foraminifera biostratigraphy. Cretaceous Research 53, 110–139. doi:
997 doi:10.1016/j.cretres.2014.11.002.

998 Frost, S. H., 1974. Cenozoic Reef Systems of Caribbean—Prospects for
999 Paleocologic Synthesis1. In: Frost, S. H., Weiss, M. P., Saunders, J. B. (eds)
1000 Reefs and Related Carbonates—Ecology and Sedimentology. American
1001 Association of Petroleum Geologists 93–110. doi: 10.1306/St4393C8.

1002 Gradstein, F. M., Ogg, J. G., Schmitz, M. D., Ogg, G. M., 2012. The Geologic
1003 Time Scale. Elsevier B.V., 1–1144 pp., doi: 10.1016/C2011-1-08249-8.

1004 Granero, P., Robles-Salcedo, R., Lucena, G., Troya, L., Vicedo, V., 2018. Els
1005 macroforaminífers i la fauna associada del Maastrichtià del sector Prebètic

1006 valencià sud (Est de la Península Ibèrica). Treballs del Museu de Geologia
1007 de Barcelona 24, 55–76. doi: <https://doi.org/10.32800/tmgb.2018.24.0055>.

1008 Greig, D. A., 1935. *Rotalia viennoti*, an important foraminiferal species from Asia
1009 Minor and western Asia. *Journal of Paleontology* 9, 523–526, pl. 1–58.

1010 Hart, M. B., Callapez, P. M., Fisher, J. K., Hannant, K., Monteiro, J. F., Price, G.
1011 D., Watkinson, M. P., 2005. Micropalaeontology and Stratigraphy of the
1012 Cenomanian/Turonian boundary in the Lusitanian Basin, Portugal. *Journal of*
1013 *Iberian Geology* 31, 311–326.

1014 Ho, Y., Zhang, P.-K., Hu, L.-Y., Sheng, J.-C., 1976. Mesozoic and Cenozoic
1015 foraminifera from the Mount Julmo Lungma Region: A reports of scientific
1016 expedition in the Mount Julmo Lungma Region (1966–1968). In: Tibetan
1017 Scientific Expeditional Team Academia Sinica. *Paleontology*. Science press,
1018 Beijing, 1–124.

1019 Hofker, J., 1959. Les Foraminifères des craies tuffoïdes de Charente et de
1020 Dordogne de l’Aquitaine, France du sud-ouest. In: 84è Congrès Des Societes
1021 Savantes, Colloque Sur Le Crétace Supérieur Français. Dijon, 253–368.

1022 Hottinger, L., 1966. Foraminifères rotaliformes et Orbitoïdes du Sénonien inférieur
1023 pyrénéen. *Eclogae Geologicae Helvetiae* 59, 277–301, pls. I–VI.

1024 Hottinger, L., 1977. Foraminifères Operculiniformes. *Mémoires du Muséum*
1025 *national d’histoire naturelle, nouv. ser.: Serie C, Sciences de la terre* 40, 1–
1026 159 pp.

1027 Hottinger, L., 2006. Illustrated glossary of terms used in foraminiferal research.
1028 *Carnets Géologie/Netbooks Geol.* 02.

- 1029 Hottinger, L. 2014. Paleogene Larger Rotaliid Foraminifera from the Western and
1030 Central Neotethys Edited by Davide Bassi. Bassi, D. (ed.). Springer, London,
1031 212 pp.
- 1032 Hottinger, L., Halicz, E., Reiss, Z. 1991. The foraminiferal genera *Pararotalia*,
1033 *Neorotalia* and *Calcarina*: taxonomic revision. *Journal of Paleontology* 65,
1034 18–33.
- 1035 Hottinger, L., Leutenegger, S., 1980. The structure of calcarinid foraminifera.
1036 *Schweizerische Paläontologische Abhandlungen* 101, 115-151.
- 1037 Kaiho, K., Hasegawa, T., 1994. End-Cenomanian benthic foraminiferal extinctions
1038 and oceanic dysoxic events in the northwestern Pacific Ocean.
1039 *Palaeogeography, Palaeoclimatology, Palaeoecology* 111, 29–43.
- 1040 Leckie, R. M., Bralower, T. J., Cashman, R., 2002. Oceanic anoxic events and
1041 plankton evolution: Biotic response to tectonic forcing during the mid-
1042 Cretaceous. *Paleoceanography* 17 (3), 13-1-13–29. doi:
1043 10.1029/2001pa000623.
- 1044 Leymerie, A., 1851. Mémoire Sur Un Nouveau Type Pyrénéen Parallèle à La Craie
1045 Proprement Dite. Gide and Baudry (eds). Paris, 26 p., XI pl.
- 1046 Luperto Sinni, E., 1976. Microfossili Senoniani delle Murge. *Rivista Italiana di*
1047 *Paleontologia e Stratigrafia* 82, 293–416.
- 1048 Luperto Sinni, E., Ricchetti, G., 1978. Studio micropaleontologico-stratigrafico di
1049 una successione carbonatica del Cretaceo superiore rilevata nel sottosuolo
1050 delle Murge sud orientali. *Rivista Italiana di Paleontologia e Stratigrafia* 84,
1051 561–666.
- 1052 Martin-Chivelet, J., 1994. Litoestratigrafía del Cretácico superior del Altiplano de
1053 Jumilla-Yecla (Zona Prebética). *Cuadernos de Geología Ibérica* 18, 117–173.

1054 Martín-Chivelet, J., 1996. Late Cretaceous subsidence history of the Betic
1055 Continental Margin (Jumilla-Yecla region, SE Spain). *Tectonophysics* 265,
1056 191–211. doi: 10.1016/S0040-1951(96)00044-3.

1057 Martín-Chivelet, J., Chacón, B., 2004. Evolución sedimentaria y paleogeográfica del
1058 Prebético: Ciclo V. In: Vera (Ed.), *Geología de España*. SGE-IGME, Madrid,
1059 369-370.

1060 Martín-Chivelet, J., Chacón, B., 2007. Event stratigraphy of the upper Cretaceous
1061 to lower Eocene hemipelagic sequences of the Prebetic Zone (SE Spain):
1062 Record of the onset of tectonic convergence in a passive continental margin.
1063 *Sedimentary Geology* 197, 141-163.
1064 <https://doi.org/10.1016/j.sedgeo.2006.09.007>.

1065 Nuttall, W. L. F., 1928. Notes on the Tertiary Foraminifera of southern Mexico.
1066 *Journal of Paleontology* 2, 372–376.

1067 Palmer, D. K., 1934. Some large fossil foraminifera from Cuba. *Memorias de la*
1068 *Sociedad Cubana de Historia Natural ‘Felipe Poey’* 8, 235-264.

1069 Papp, A. Von., 1955. Orbitoiden aus der Oberkreide der Ostalpen
1070 (Gosauschichten). *Sitzungsberichten der Österreichischen Akademie der*
1071 *Wissenschaften, Wien, Mathematisch-Naturwissenschaftliche Klasse* 164,
1072 303–315.

1073 Parente, M., Frijia, G., Lucia, M. di., 2007. Carbon-isotope stratigraphy of
1074 Cenomanian–Turonian platform carbonates from the southern Apennines
1075 (Italy): a chemostratigraphic approach to the problem of correlation between
1076 shallow-water and deep-water successions. *Journal of the Geological Society*
1077 163, 609–620. doi: 10.1144/0016-76492006-010.

1078 Parente, M., Frijia, G., Lucia, M. Di, Jenkyns, H. C., Woodfine, R. G., Baroncini,
1079 F., 2008. Stepwise extinction of larger foraminifers at the Cenomanian–
1080 Turonian boundary: A shallow-water perspective on nutrient fluctuations
1081 during Oceanic Anoxic Event 2 (Bonarelli Event). *Geology* 36, 715–718. doi:
1082 10.1130/G24893A.1.

1083 Poignant, A., 1998. Révision des espèces de foraminifères signalées par
1084 d’Orbigny en Aquitaine (S.O. France) dans le ‘Tableau méthodique de la
1085 classe des Céphalopodes’ (1826). *Revue de Micropaléontologie* 41, 107–149.

1086 Poignant, A., Pujol, C., 1978. Nouvelles données micropaléontologiques
1087 (foraminifères planctoniques et petits foraminifères benthiques) sur le stratotype
1088 bordelais du Burdigalien. *Géobios* 11, 655–712.

1089 Pons, J. M., Gallemí, J., Höfling, R., Moussavian, E., 1994. *Los Hippurites* del
1090 Barranc del Racó, microfacies y fauna asociada (Maastrichtiense Superior, sur
1091 de la provincia de Valencia). *Cuadernos de Geología Ibérica* 18, 271–307.

1092 Pons, J. M., Vicens, E., 2002. Campanian and Maestrichtian rudists from southern
1093 Valencia province, South East Spain. In: *Proc. 1st International Conference*
1094 *on Rudists*, UGSY, Mem. Publ. 233–263.

1095 Rahaghi, A., 1976. Contribution à l’étude de quelques grands foraminifères de
1096 l’Iran. *Publications de la Société National Iranienne des Pétroles, Laboratoire*
1097 *de Micropaléontologie, Tehran*, 6, 1–79.

1098 Ramírez del Pozo, J., Martín-Chivelet, J., 1994. Bioestratigrafía y
1099 cronoestratigrafía del Coniaciense–Maastrichtiense en el sector Prebético de
1100 Jumilla-Yecla (Murcia). *Cuadernos de Geología Ibérica* 18, 83–116.

1101 Raup, D. M., Sepkoski Jr., J. J., 1986. Periodic extinction of families and genera.
1102 *Science* 231, 833–836.

- 1103 Reuss, A. E., 1862. Sitzungsberichte der Kaiserlichen Akademie der
1104 Wissenschaften. Mathematisch-Naturwissenschaftliche Classe 44, 301–342.
- 1105 Robles-Salcedo, R., 2014. La Familia Siderolitidae (Macroforaminíferos Del
1106 Cretácico Superior): Arquitectura de La Concha, Bioestratigrafía,
1107 Distribución Paleoambiental y Paleobiogeografía. Universitat Autònoma de
1108 Barcelona, Barcelona, 183 pp.
1109 <http://global.tesisenred.net/handle/10803/285038>.
- 1110 Robles-Salcedo, R., Vicedo, V., 2016. Bioestratigrafía con macroforaminíferos
1111 hialinos del Cretácico superior de la Zona Prebética Externa norte, in: Morales
1112 González, J. A. (ed.) IX Congreso Geológico de España - Geo-Temas. Geo-
1113 Temas, Huelva, 257–260.
- 1114 Robles-Salcedo, R., Rivas, G., Vicedo, V., Caus, E., 2013. Paleoenvironmental
1115 distribution of larger foraminifera in Upper Cretaceous siliciclastic-carbonate
1116 deposits (Arén Sandstone Formation, south Pyrenees, northeastern Spain).
1117 *Palaios* 28, 637–648. doi: <http://dx.doi.org/10.2110/palo.2012.p12-125r>.
- 1118 Robles-Salcedo, R., Vicedo, V., Caus, E., 2018. Latest Campanian and
1119 Maastrichtian Siderolitidae (larger benthic foraminifera) from the Pyrenees (S
1120 France and NE Spain). *Cretaceous Research* 81, 64–85. doi:
1121 [10.1016/j.cretres.2017.08.017](https://doi.org/10.1016/j.cretres.2017.08.017).
- 1122 Robles-Salcedo, R., Vicedo, V., Parente, M., Caus, E., 2019. *Canalispina iapygia*
1123 gen. et sp. nov.: the last Siderolitidae (Foraminiferida) from the upper
1124 Maastrichtian of southern Italy. *Cretaceous Research* 98, 84–94. doi:
1125 [10.1016/j.cretres.2019.01.009](https://doi.org/10.1016/j.cretres.2019.01.009).

1126 Schlumberger, C., 1900. Note sur quelques Foraminifères nouveaux ou peu connus
1127 du Crétacé d'Espagne. Bulletin de la Société géologique de France 3, 456–
1128 465.

1129 Schlüter, M., Steuber, T., Parente, M., 2008. Chronostratigraphy of Campanian–
1130 Maastrichtian platform carbonates and rudist associations of Salento (Apulia,
1131 Italy). Cretaceous Research 29, 100–114. doi: 10.1016/j.cretres.2007.04.005.

1132 Seiglie, G. A., Ayala-Castañares, A., 1963. Sistemática y bioestratigrafía de los
1133 foraminíferos grandes del Cretácico Superior (Campaniano y Maastrichtiano)
1134 de Cuba. Paleontología Mexicana 13, 1–56.

1135 Silva, I. P., Sliter, W. V., 1999. Cretaceous paleoceanography: evidence from
1136 planktonic foraminiferal evolution, in: Barrera, E. and Johnson, C. C. (eds)
1137 Evolution of the Cretaceous Ocean-Climate System. Geological Society of
1138 America. doi: <https://doi.org/10.1130/SPE332>.

1139 Silvestri, A., 1940. Illustrazione di specie caratteristica del Cretaceo superiore.
1140 Bollettino della Società Geologica Italiana 58, 225–234.

1141 Sirel, E., 1972. Systematic Study of New Species of The Genera *Fabularia* and
1142 *Kathina* from Paleocene. Türkiye Jeoloji Bülteni 15, 277–294.

1143 Sirel, E., 2012. Seven new larger benthic foraminiferal genera from the Paleocene
1144 of Turkey. Revue de Paléobiologie 31, 267–301.

1145 Solak, C., Tash, K., Koç, H., 2017. Biostratigraphy and facies analysis of the
1146 Upper Cretaceous–Danian? platform carbonate succession in the Kuyucak
1147 area, western Central Taurides, S Turkey. Cretaceous Research 79, 43–63.
1148 doi: 10.1016/j.cretres.2017.06.019.

1149 Tentor, A., 2007. Stratigraphic observations on Mount Brestovi (Karst of Gorizia,
1150 Italy). Natura Nascosta 35, 1–23.

- 1151 Thalmann, H. E., 1939. Mitteilungen über Foraminiferen IV. *Eclogae Geologicae*
1152 *Helvetiae* 31, 327–332.
- 1153 Thiadens, A. A., 1937. Cretaceous and Tertiary Foraminifera from southern Santa
1154 Clara Province, Cuba. *Journal of Paleontology* 11, 91–109.
- 1155 Torre, M., 1967. Alcuni foraminiferi del Cretacico. *Bollettino della Società di*
1156 *naturalisti in Napoli* 75, 409–431.
- 1157 Uhlig, V., 1886. Über eine Mikrofauna aus dem Alttertiär der westgalizischen
1158 Karpathen. *Jahrbuch der K. K. Geologischen Reichsanstalt, Wien* 36, 141–
1159 214.
- 1160 Vaughan, T. W., 1945. Part I.- American Paleocene and Eocene larger
1161 Foraminifera. *Geological Society of America* 9, 1–175, pls. 1–46.
- 1162 Vera, J. (ed.), 2004. *Geología de España*. SGE-IGME, Madrid, 890 pp.
- 1163 Vera, J. A., Garcia-Hernández, M., López-Garrido, A. C., Comas, M. C., Ruiz-
1164 Oniz, P. A., Martin-Algarra, A., 1982. La Cordillera Bética, in: *El Cretácico*
1165 *de España*. Universidad Complutense, Madrid, 515–632.
- 1166 Vicedo, V., 2009. *Morfoestructura de Los Géneros Cretácicos de Los*
1167 *Rhapydioninidae (Foraminifera)*. Universitat Autònoma de Barcelona,
1168 Barcelona, 171 pp.
- 1169 Vicedo, V., Robles-Salcedo, R., Hidalgo, C., Razin, P., Elaud, C. G. R., 2019.
1170 *Biostratigraphy and evolution of larger rotaliid foraminifera in the Cretaceous*
1171 *– Palaeogene transition of the southern Oman Mountains*. *Papers in*
1172 *Paleontology* 7(1) 1–26, doi: <https://doi.org/10.1002/spp2.1281>.
- 1173 Vilas, L., Martín-Chivelet, J., Arias, C., 2003. Integration of subsidence and
1174 sequence stratigraphic analyses in the Cretaceous carbonate platforms of the

1175 Prebetic (Jumilla-Yecla Region), Spain. *Palaeogeography, Palaeoclimatology,*
1176 *Palaeoecology* 1-4, 107–129. doi: 10.1016/S0031-0182(03)00447-4.

1177 Villalonga, R., Boix, C., Frijia, G., Parente, M., Bernaus, J. M., Caus, E., 2019.
1178 Larger foraminifera and strontium isotope stratigraphy of middle Campanian
1179 shallow-water lagoonal facies of the Pyrenean Basin (NE Spain). *Facies* 65,
1180 1–23. doi: 10.1007/s10347-019-0569-0.

1181 Visser, A. M., 1951. Monograph on the foraminifera of the type-locality of the
1182 Maestrichtian (South-Limburg, Netherlands). *Leidse Geologische*
1183 *Mededelingen* 16, 197–359.

1184 Voorwijk, G. H., 1937. Foraminifera from the Upper Cretaceous of Habana. K.
1185 *Akad. Wetensch. Amsterdam Verh.* 40, 190–198, pls. 1–3.

1186 Wannier, M., 1980. La structure des Siderolitinae, foraminifères du Crétacé
1187 supérieur. *Eclogae Geologicae Helvetiae* 73(3), 1009-1029.

1188 Wannier, M., 1983. Evolution, biostratigraphie et systematique des Siderolitinae
1189 (Foraminiferes). *Revista Española de Micropaleontología* 15, 5–37.

1190

1191

1192

1193 **Figure captions**

1194 **Figure 1.** Geographical location of the stratigraphical sections and the two outcrops.

1195 **Figure 2.** Stratigraphic succession and distribution of larger foraminifera and other
1196 fossil groups in the Serra de la Solana section, Bocairent (Valencia, Spain).

1197 **Figure 3.** Stratigraphic succession and distribution of larger foraminifera and other
1198 fossil groups in the Serra Grossa section, Ontinyent (Valencia, Spain).

1199 **Figure 4.** Stratigraphic succession and distribution of larger foraminifera and other
1200 fossil groups in the Penya del Romaní Hill section, SE of Serra del Buixcarró, Pinet
1201 (Valencia, Spain).

1202 **Figure 5.** Stratigraphic succession and distribution of larger foraminifera and other
1203 fossil groups in the Serra de les Agulles section, Benifairó de la Valldigna (Valencia,
1204 Spain).

1205 **Figure 6.** *Pseudosulcoperculina bocairentina* gen. et sp. nov. from the Maastrichtian
1206 deposits of Serra de la Solana, Bocairent (Valencia, Spain). Transmitted light
1207 photographs of thin sections of cemented carbonate rocks. Scale bar 500 µm. A–E and
1208 G–U, paratypes. F, holotype. *Abbreviations:* ft, feathering; fu, funnel; p, proloculus; pg,
1209 umbilical plug; pi, pile; s, septum; spc, spiral canal; su, sulcus; up, umbilical plate. The
1210 accession numbers from A to U are 64072 LP16.008; 84627 LP01.008; 64072
1211 LP08.002; 84627 LP01.009; 64072 LP03.011; 69778 LP05.005; 64072 LP14.021;
1212 64072 LP03.013; 64072 LP19.008; 64072 LP03.002; 64072 LP13.013; 64072
1213 LP08.012; 64072 LP21.002; 64072 LP01.005; 64072 LP06.010; 64072 LP14.004;
1214 64072 LP13.002; 64072 LP17.004; 84632 LP02.003; 64072 LP01.010; 64072
1215 LP07.009, respectively, all of them under the acronym MGB.

1216 **Figure 7.** *Pseudosulcoperculina bocairentina* gen. et sp. nov. from the Maastrichtian
1217 deposits of Serra de la Solana, Bocairent (Valencia, Spain). Transmitted light
1218 photographs of thin sections of cemented carbonate rocks. Scale bar 500 μm . All the
1219 specimens are paratypes. *Abbreviations:* foa, foliar aperture; ft, feathering; ic, intraseptal
1220 canal; pg, umbilical plug; spc, spiral canal; su, sulcus; up, umbilical plate. The
1221 accession numbers from A to L are 69778 LP04.030; 64072 LP13.008; 64072
1222 LP14.003; 64072 LP04.002; 64072 LP01.009; 62072 LP03.010; 64072 LP11.011;
1223 69950 LP01.018; 64072 LP16.001; 64072 LP14.005; 69950 LP01.016; 84627
1224 LP01.002, respectively, all of them under the acronym MGB.

1225 **Figure 8.** **A–E**, *Pseudosulcoperculina bocairentina* gen. et sp. nov.; **F–G**,
1226 *Plumopraeolockhartia solanensis* gen. et sp. nov.; **H**, and *Pararotalia tuberculifera*
1227 (Reuss, 1862) from the Maastrichtian deposits of Serra del Regalí (Albacete, Spain).
1228 Transmitted light photographs of thin sections of cemented carbonate rocks. Scale bar
1229 500 μm . *Abbreviations:* ft, feathering; fu, funnel; pi, pile; su, sulcus; uc, umbilical
1230 cavity; upc, umbilical peripheral cavity. The accession numbers from A to H are 84665
1231 LP03.001; 84666 LP01.005; 84665 LP01.008; 84666 LP01.002; 84666 LP02.001;
1232 84666 LP01.004; 84665 LP01.009; 84665 LP01.002, respectively, all of them under the
1233 acronym MGB.

1234 **Figure 9.** *Pseudosulcoperculina* sp. from the lower Maastrichtian deposits of the south
1235 Pyrenees (Lleida, Spain). Transmitted light photographs of thin sections of cemented
1236 carbonate rocks. Scale bar 500 μm . The accession numbers from A to D are 82546
1237 LP01.001; 82547 LP01.001; 82548 LP01.001; 82549 LP01.001, respectively, all of
1238 them under the acronym MGB.

1239 **Figure 10.** *Plumopraelockhartia solanensis* gen. et sp. nov. from the Maastrichtian
1240 deposits of Serra de la Solana, Bocairent (Valencia, Spain). Transmitted light
1241 photographs of thin sections of cemented carbonate rocks. Scale bar 500 μ m. A, C–V,
1242 paratypes. B, holotype. *Abbreviations:* do, dorsal ornamentation; f, foramen; foa, foliar
1243 aperture; ft, feathering; fu, funnel; is, interocular intraseptal space; n, notch; p,
1244 proloculus; pi, pile; s, septum; uc, umbilical cavity; up, umbilical plate; upc, umbilical
1245 peripheral cavity. The accession numbers from A to V are 64072 LP01.012; 84627
1246 LP01.004; 64072 LP11.007; 64072 LP07.004; 64072 LP11.013; 64072 LP01.034;
1247 64072 LP14.011; 84633 LP01.003; 64072 LP14.018; 69950 LP01.013; 84633
1248 LP01.001; 64072 LP17.020; 64072 LP15.022; 64072 LP18.018; 84632 LP02.013;
1249 64072 LP03.009; 64072 LP17.023; 84633 LP01.002; 64072 LP18.018; 84627
1250 LP01.005; 84629 LP01.009; 69778 LP04.021, respectively, all of them under the
1251 acronym MGB.

1252 **Figure 11.** *Rotalispira scarsellai* (Torre, 1966) from the upper Campanian deposits of
1253 Serra Grossa, Ontinyent (Valencia, Spain). Transmitted light photographs of thin
1254 sections of cemented carbonate rocks. Scale bar 500 μ m. *Abbreviations:* f, foramen; fo,
1255 folium; s, septum. The accession numbers from A to X are 69816 LP02.009; 69817
1256 LP03.057; 69817 LP01.051; 69817 LP02.060; 69817 LP02.047; 69817 LP01.070;
1257 69817 LP02.064; 69817 LP02.062; 69817 LP02.073; 69816 LP01.053; 69816
1258 LP01.058; 69817 LP01.063; 69817 LP01.054; 69816 LP01.056; 69817 LP01.055;
1259 69817 LP01.073; 69817 LP02.053; 69817 LP02.044; 69816 LP02.001; 69816
1260 LP01.057; 69817 LP01.052; 69817 LP01.062; 69817 LP01.064; 69817 LP02.061,
1261 respectively, all of them under the acronym MGB.

1262 **Figure 12.** *Rotalia baetica* sp. nov. from the upper Campanian deposits of Peña del
1263 Romaní Hill, SE of Serra del Buixcarró, Pinet (Valencia, Spain). Transmitted light

1264 photographs of thin sections of cemented carbonate rocks. Scale bar 500 μ m. A–D, F–
1265 R, paratypes. E, holotype. *Abbreviations*: col, columella; f, foramen; fo, folium; s,
1266 septum; up, umbilical plate. The accession numbers from A to R are 60322 LP18.002;
1267 69733 LP06.002; 60323 LP02.001; 69735 LP06.002; 60323 LP03.007; 69737
1268 LP07.001; 60322 LP06.010; 60323 LP01.001; 60321 LP09.003; 60319 LP02.002;
1269 60322 LP07.007; 69734 LP10.005; 60324 LP01.013; 60322 LP11.001; 60321
1270 LP04.002; 60322 LP14.003; 60321 LP06.009; 62321 LP04.001, respectively, all of
1271 them under the acronym MGB.

1272 **Figure 13.** -*Rotorbinella* sp. from the upper Campanian deposits of Penya del Romaní
1273 Hill, SE of Serra del Buixcarró, Pinet. Transmitted light photographs of thin sections of
1274 cemented carbonate rocks. Scale bar 500 μ m. *Abbreviations*: p, proloculus; pg,
1275 umbilical plug; s, septum. The accession numbers from A to F are 60323 LP03.002;
1276 60323 LP03.006; 60322 LP14.002; 60322 LP14.005; 69734 LP09.003; 60323
1277 LP03.008, respectively, all of them under the acronym MGB.

1278 **Figure 14.** *Suturina minima* sp. nov. from the upper Campanian deposits of Penya del
1279 Romaní Hill, SE of Serra del Buixcarró, Pinet (Valencia, Spain). Transmitted light
1280 photographs of thin sections of cemented carbonate rocks. Scale bar 250 μ m. A, B, D–
1281 T, paratypes. C, holotype. *Abbreviations*: f, foramen; fo, folium; n, notch; s, septum; up,
1282 umbilical plate. The accession numbers from A to T are 60335 LP02.040; 60335
1283 LP03.009; 60335 LP02.036; 60335 LP02.044; 60334 LP05.013; 60335 LP02.045;
1284 60335 LP03.006; 60335 LP01.007; 60334 LP05.001; 60334 LP02.006; 60334
1285 LP05.010; 60335 LP03.010; 60334 LP02.007; 60335 LP02.027; 60334 LP02.008;
1286 60334 LP05.008; 60335 LP02.031; 60330 LP02.005; 60334 LP05.013; 60335
1287 LP02.032, respectively, all of them under the acronym MGB.

1288 **Figure 15.** *Suturina minima* sp. nov. from the upper Campanian deposits of Peña del
1289 Romaní Hill, SE of Serra del Buixcarró, Pinet (Valencia, Spain). Transmitted light
1290 photographs of thin sections of cemented carbonate rocks. Scale bar 250 µm. All the
1291 specimens are paratypes. *Abbreviations:* f, foramen; fo, folium; foa, foliar aperture; ic,
1292 intraseptal canal; n, notch; s, septum; spc, spiral canal; up, umbilical plate. The
1293 accession numbers from A to Q are 60334 LP05.002; 60334 LP05.012; 60334
1294 LP02.010; 60334 LP05.011; 60335 LP02.033; 60335 LP01.005; 60335 LP01.011;
1295 60335 LP01.006; 60334 LP02.006; 60335 LP01.008; 60334 LP02.011; 60335
1296 LP01.008; 60335 LP01.010; 60335 LP01.009; 60334 LP02.004; 60335 LP01.001;
1297 60335 LP02.041, respectively, all of them under the acronym MGB.

1298 **Figure 16.** *Suturina minima* sp. nov. from the upper Campanian deposits of Peña del
1299 Romaní Hill, SE of Serra del Buixcarró, Pinet (Valencia, Spain). Transmitted light
1300 photographs of thin sections of cemented carbonate rocks. Scale bar 250 µm. All the
1301 specimens are paratypes. *Abbreviations:* f, foramen; fo, folium; s, septum; up, umbilical
1302 plate. The accession numbers from A to H are 60334 LP04.008; 60334 LP04.009;
1303 60334 LP04.006; 60334 LP04.007; 60334 LP04.001; 60334 LP03.006; 60334
1304 LP03.002; 60334 LP03.001, respectively, all of them under the acronym MGB.

1305 **Figure 17.** *Suturina minima* sp. nov. (A–H) and *Suturina globosa* Consorti, Vilallonga
1306 and Caus, 2017 (I–K) from the upper Campanian deposits of Serra Grossa, Ontinyent
1307 (Valencia, Spain). Transmitted light photographs of thin sections of cemented carbonate
1308 rocks. Scale bar 500 µm. The accession numbers from A to K are 69833 LP01.010;
1309 69843 LP01.028; 69833 LP01.005; 69818 LP01.002; 69830 LP01.001; 69843
1310 LP01.026; 69843 LP01.022; 69811 LP01.001, 69817 LP03.058; 69817 LP01.066;
1311 69817 LP02.075, respectively, all of them under the acronym MGB.

1312 **Figure 18.** *Neorotalia? pinetensis* sp. nov. from the upper Campanian deposits of Penya
1313 del Romaní Hill, SE of Serra del Buixcarró, Pinet (Valencia, Spain). Transmitted light
1314 photographs of thin sections of cemented carbonate rocks. Scale bar 500 µm. A, C–X,
1315 paratype. B, holotype. *Abbreviations:* f, foramen; fu, funnel; is, interocular intraseptal
1316 space; p, proloculus; pi, pile; tp, toothplate. The accession numbers from A to X are
1317 60316 LP03.002; 60316 LP04.005; 60316 LP03.008; 60316 LP03.014; 60316
1318 LP05.001; 60316 LP03.011; 60316 LP01.014; 60319 LP01.008; 60316 LP06.006;
1319 60316 LP04.004; 60316 LP05.006; 60316 LP04.003; 60316 LP06.004; 60316
1320 LP05.007; 60316 LP03.013; 60316 LP04.002; 60318 LP02.004; 60316 LP05.010;
1321 60318 LP02.006; 60316 LP03.012; 60316 LP06.001; 60318 LP02.002; 60316
1322 LP06.005; 60318 LP02.007, respectively, all of them under the acronym MGB.

1323 **Figure 19.** *Neorotalia? pinetensis* sp. nov. from the upper Campanian deposits of Serra
1324 de les Agulles, Benifairó de la Valldigna (Valencia, Spain). Transmitted light
1325 photographs of thin sections of cemented carbonate rocks. Scale bar 500 µm.
1326 *Abbreviations:* f, foramen; is, interocular intraseptal space; spc, spiral canal; tp,
1327 toothplate. The accession numbers from A to D are 60354 LP01.001; 60354 LP01.002;
1328 60356 LP01.001; 60357 LP01.002, respectively, all of them under the acronym MGB.

1329 **Figure 20.** *Pararotalia tuberculifera* (Reuss, 1862). **A–J**, specimens from the upper
1330 Campanian deposits of Penya del Romaní Hill, SE of Serra del Buixcarró, Pinet; **K–N**,
1331 specimens from the upper Maastrichtian deposits of Serra de la Solana, Bocarent.
1332 Transmitted light photographs of thin sections of cemented carbonate rocks. Scale bar
1333 500 µm. *Abbreviations:* pg, umbilical plug. The accession numbers from A to N are
1334 69733 LP05.004; 69737 LP06.004; 69733 LP05.002; 69736 LP06.004; 69733
1335 LP05.003; 69733 LP01.003; 60324 LP01.012; 60322 LP01.008; 69736 LP11.002;

1336 60322 LP08.001; 64072 LP13.010; 64072 LP03.023; 64072 LP17.011; 64072
1337 LP06.009, respectively, all of them under the acronym MGB.

1338 **Figure 21.** Selected larger foraminifera from the late Campanian deposits of Penya del
1339 Romaní Hill, SE of Serra del Buixcarró, Pinet (Valencia, Spain). Transmitted light
1340 photographs of thin sections of cemented carbonate rocks. Scale bar: 500 µm for A, C,
1341 E–K and M, 1 mm for B, D and L. **A**, *Cuneolina cylindrica* Henson; **B**, *Haddonina* sp.
1342 encrusted with *Polystrata alba* (Pfender) Denizot (aragonitic red coralline algae); **C**,
1343 *Nummofallotia cretacea* (Schlumberger); **D**, *Orbitoides* cf. *media* (d'Archiac); **E**,
1344 “*Orbitoides*” cf. *concavatus* Rahaghi; **F**, *Praesiderolites douvillei* Wannier; **G**,
1345 *Lepidorbitoides* cf. *campaniensis* van Gorsel; **H**, *Stomatorbina binkhorsti* (Reuss); **I**,
1346 *Wannierina* cf. *vilavellensis* Robles-Salcedo, Vicedo and Caus; **J**, *Sirtina ornata*
1347 (Rahaghi); **K**, *Planorbulina cretae* (Marsson); **L**, *Pseudosiderolites vidali* (Douvillé);
1348 **M**, aff. *Sivasella* sp. The accession numbers from A to M are 60330 LP01.001; 69732
1349 LP07.001; 60322 LP01.007; 60322 LP01.018; 60324 LP02.005; 60324 LP01.006;
1350 69734 LP02.004; 60319 LP08.005; 60329 LP01.003; 60322 LP01.012; 60322
1351 LP04.002; 60324 LP14.002; 60323 LP02.005, respectively, all of them under the
1352 acronym MGB.

1353

1354 **Figure 22.** Selected larger foraminifera from the upper Campanian deposits of Serra de
1355 les Agulles, Benifairó de la Valldigna (Valencia, Spain). Transmitted light photographs
1356 of thin sections of cemented carbonate rocks. Scale bar: 1 mm for A–C, 500 µm for D–
1357 I. **A**, *Orbitoides* sp.; **B**, *Arnaudiella grossouvrei*
1358 Douvillé; **C**, *Lepidorbitoides* sp.; **D**, *Praesiderolites*
1359 *douvillei* Wannier; **E**, *Goupillaudina shirazensis* Rahaghi; **F**, *Nummofallotia*
1360 *cretacea* (Schlumberger); **G**, *Idalina antiqua* Schlumberger & Munier-Chalmas; **H**,

1361 *Praestorrsella roestae* (Visser); **I**, Textulariid. The accession numbers from A to I are
1362 60354 LP01.010; 60356 LP01.002; 60367 LP01.002; 60344 LP01.002; 60345
1363 LP01.001; 60354 LP01.012; 60354 LP01.009; 60344 LP01.004; 60344 LP01.001,
1364 respectively, all of them under the acronym MGB.

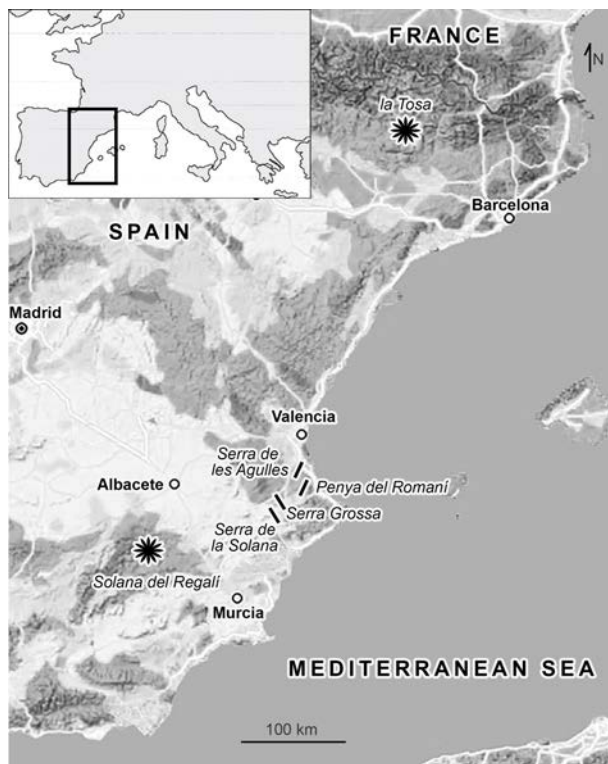
1365

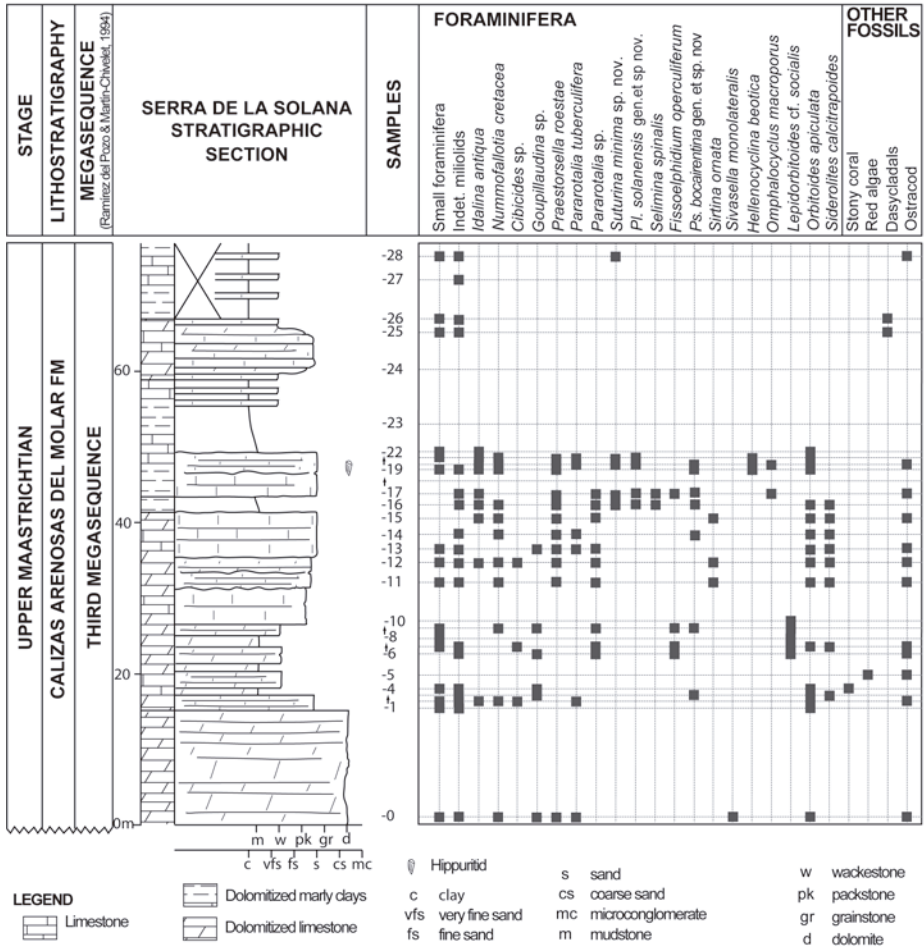
1366 **Figure 23.** Selected larger foraminifera from late Campanian deposits of Serra Grossa,
1367 Ontinyent (Valencia, Spain). Transmitted light photographs of thin sections of cemented
1368 carbonate rocks. Scale bars: A–D, 200 μm , E–G, I, 500 μm , H, J, 1 mm. **A**, *Fleuryana*
1369 sp.; **B**, *Nezzazatinella* sp.; **C**, *Murgeina apula* (Luperto Sinni); **D**, *Dictyopsella* sp.; **E**,
1370 *Scandonea* sp.; **F**, *Cuneolina cylindrica* Henson; **G**, *Praseiderolites douvillei* Wannier;
1371 **H**, *Orbitoides* cf. *media* (d'Archiac); **I**, *Murciella* aff. *cuvillieri* Fourcade (M) and
1372 *Cuvillierinella* cf. *salentina* Papetti and Tedeschi (C); **J**, *Pseudosiderolites vidali*
1373 (Douvillé). The accession numbers from A to J are 69817 LP02.070; 69817 LP03.009;
1374 69833 LP01.004; 69822 LP01.003; 69812 LP01.001; 69816 LP01.001; 69822
1375 LP01.001; 69823 LP01.001; 69817 LP03.024; 69817 LP03.025; 69819 LP01.006,
1376 respectively, all of them under the acronym MGB.

1377

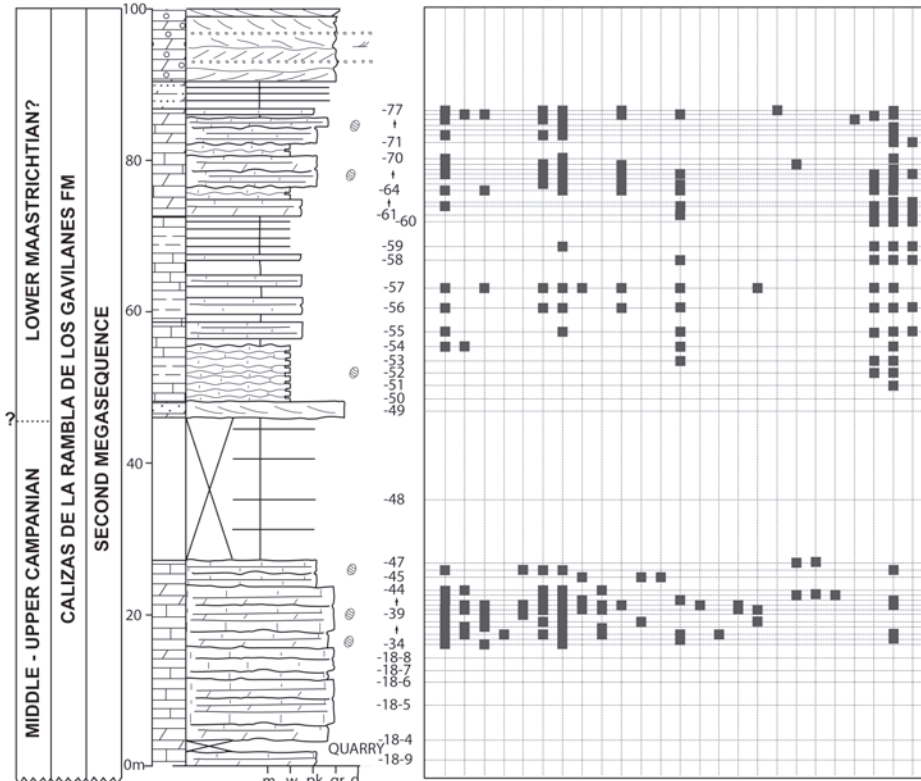
1378 **Figure 24.** Selected larger foraminifera from the upper Maastrichtian deposits of Serra
1379 de la Solana, Bocairent (Valencia, Spain). Transmitted light photographs of thin
1380 sections of cemented carbonate rocks. Scale bars: A–C, 1 mm, D–K, 500 μm . **A**,
1381 *Omphalocyclus macroporus* (Lamarck); **B**, *Orbitoides apiculata* Schlumberger; **C**,
1382 *Orbitoides gensacicus* (Leymerie); **D**, *Hellenocyclina beotica* Reichel; **E**, *Selimina*
1383 *spinalis* Inan; **F**, *Sivasella monolateris* Sirel and Gündüz; **G**, *Idalina antiqua*
1384 Schlumberger and Munier-Chalmas; **H**, *Nummofallotia cretacea* (Schlumberger); **I**,
1385 *Fissoelphidium operculiferum* Smout; **J**, *Sirtina orbitoidiformis* Brönnimann and Wirz;

- 1386 **K**, *Siderolites calcitrapoides* Lamarck. The accession numbers from A to K are 64072
1387 LP17.002; 64072 LP03.001; 64072 LP05.002; 64072 LP01.023; 84627 LP01.018;
1388 67870 LP01.001; 67891 LP01.001; 67885 LP01.002; 64072 LP15.004; 64072
1389 LP02.007; 84632 LP01.004, respectively, all of them under the acronym MGB.
- 1390
- 1391
- 1392



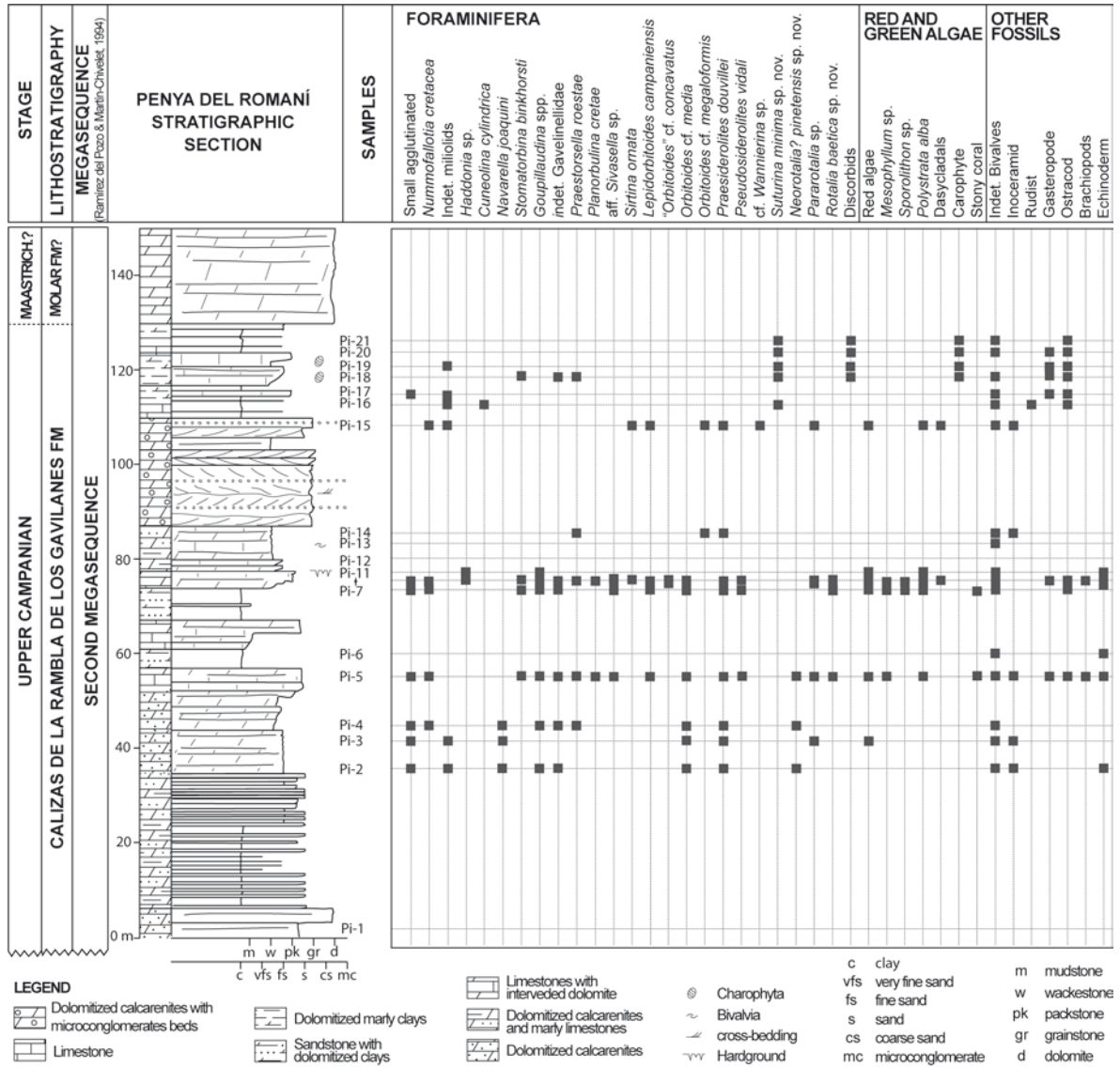


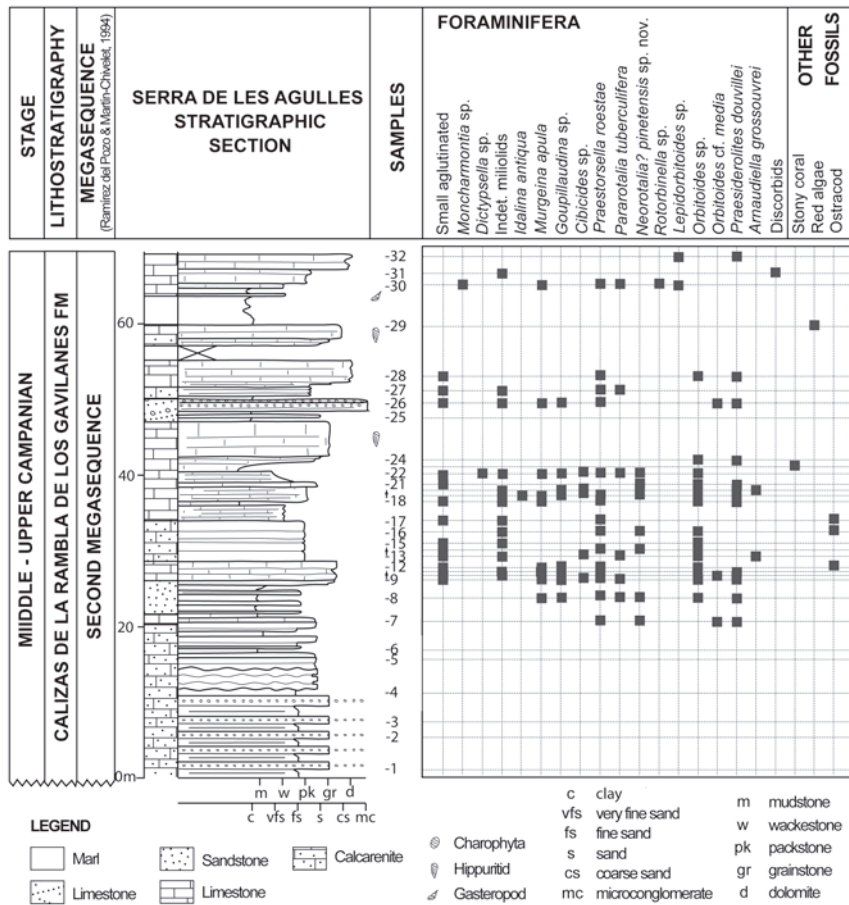
STAGE	LITHOSTRATIGRAPHY	SERRA GROSSA STRATIGRAPHIC SECTION	SAMPLES	FORAMINIFERA
	MEGASEQUENCE <small>(Ramirez del Pozo & Martín-Chivelet, 1994)</small>			

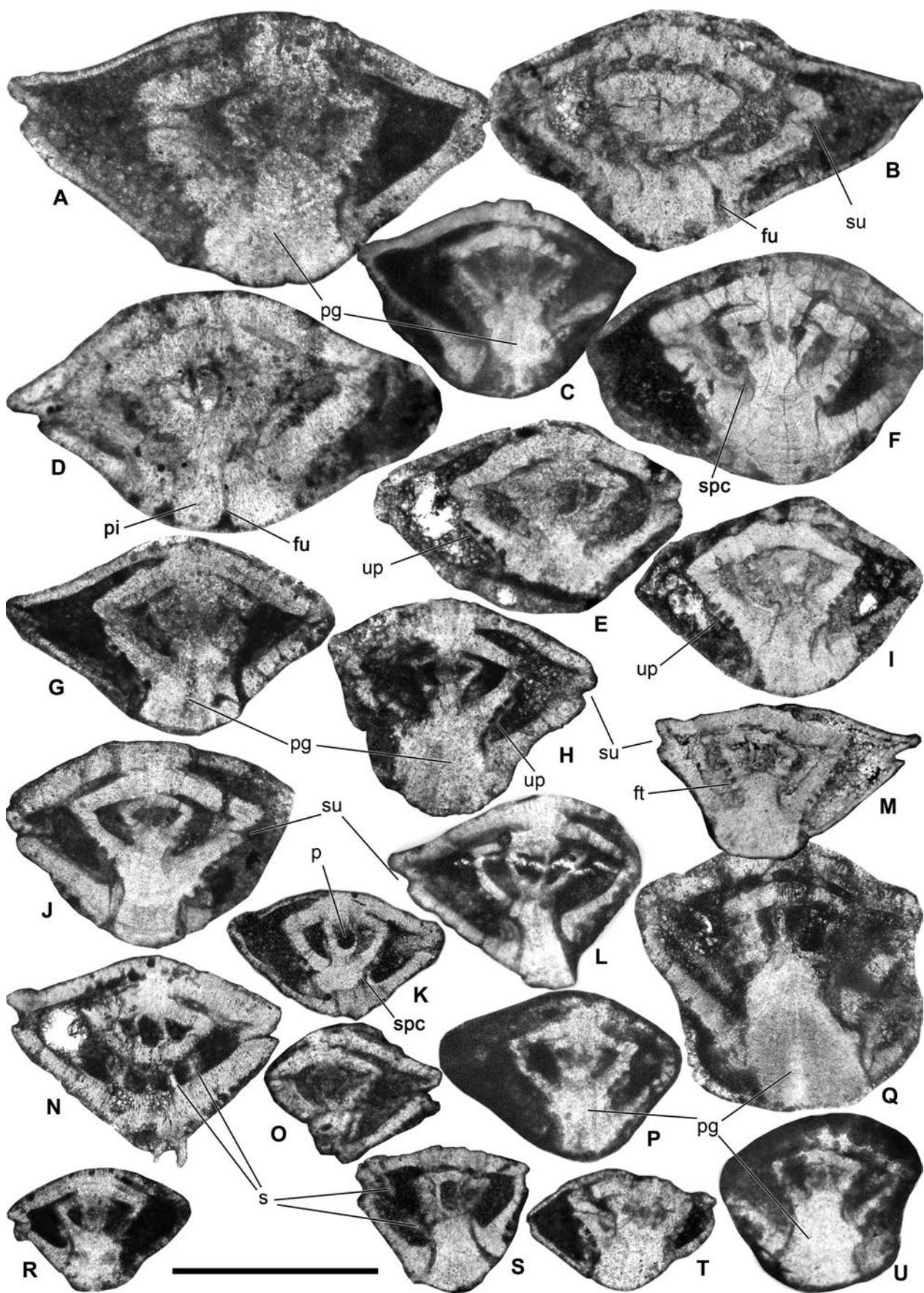


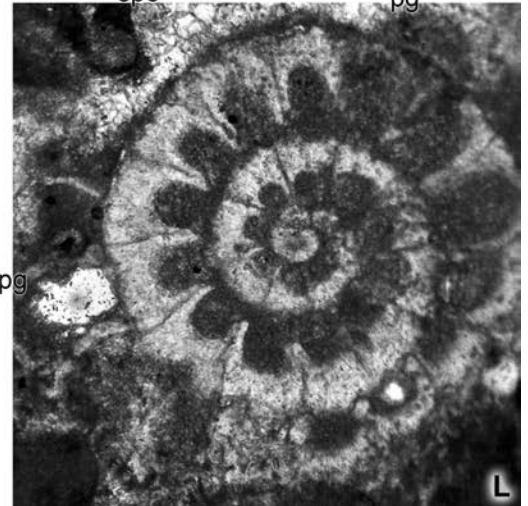
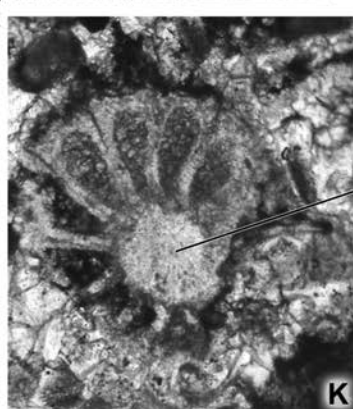
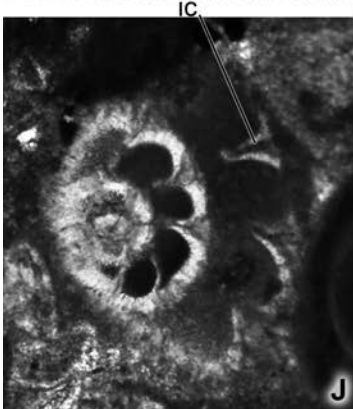
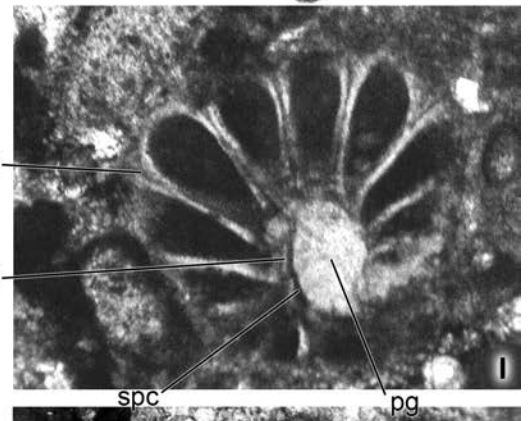
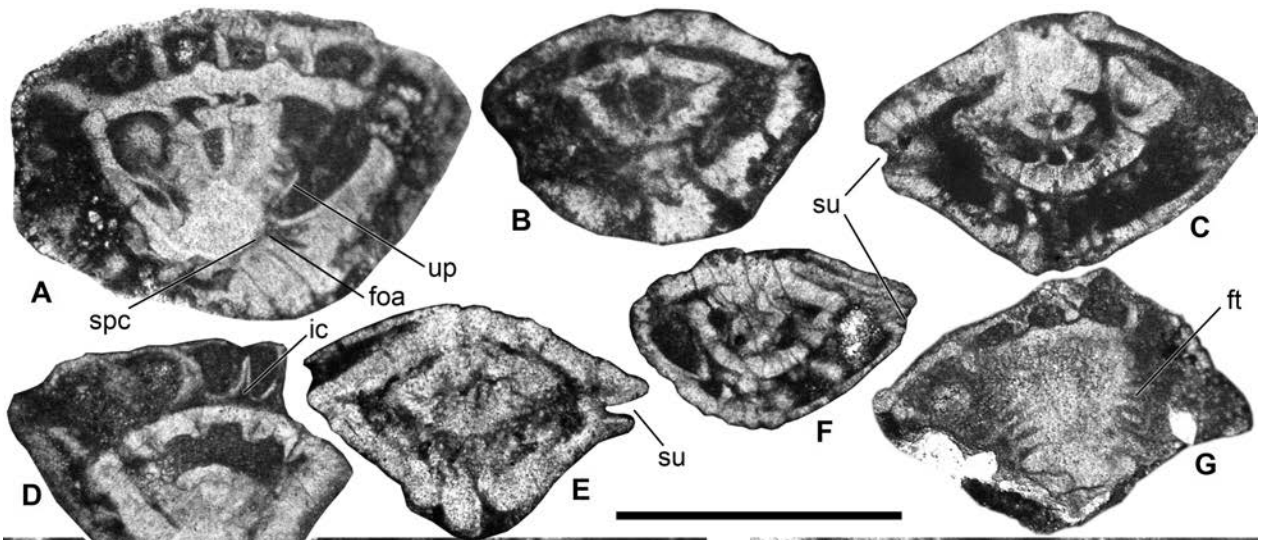
LEGEND			
Dolomitized calcarenites with microconglomerates beds	Marl	Limestones with interbedded dolomite	Charophyta
Limestone	Sandstone with dolomitized clays	Marly clays	cross-bedding
			clay
			very fine sand
			fine sand
			sand
			coarse sand
			microconglomerate
			mudstone
			wackestone
			packstone
			grainstone
			dolomite

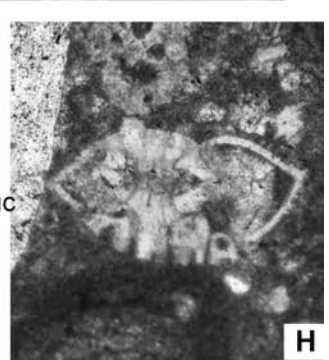
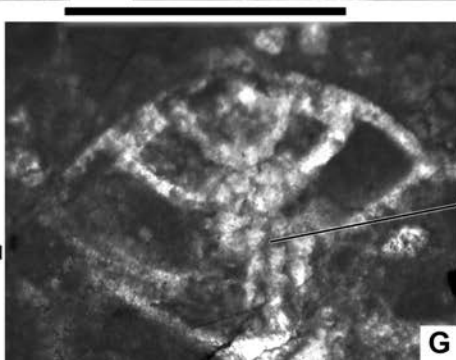
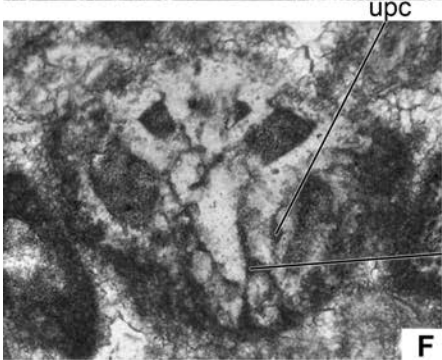
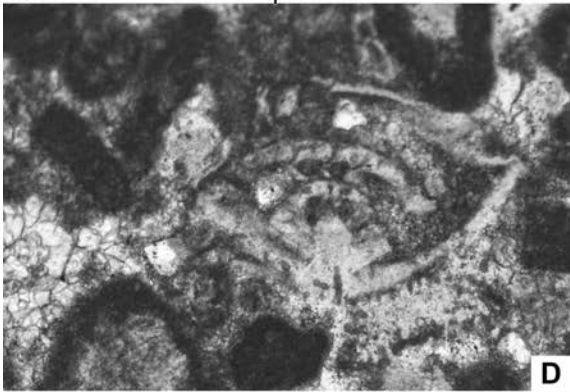
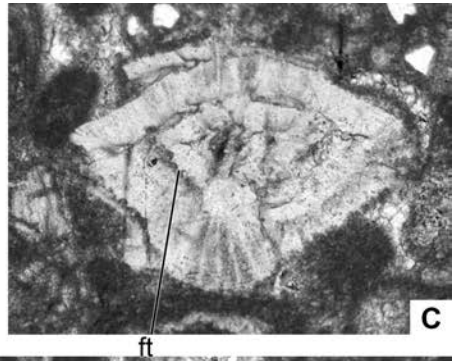
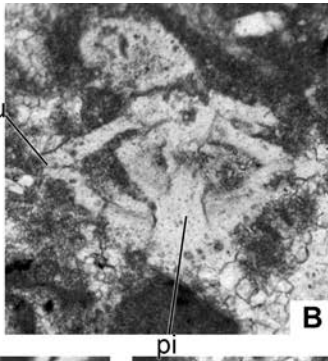
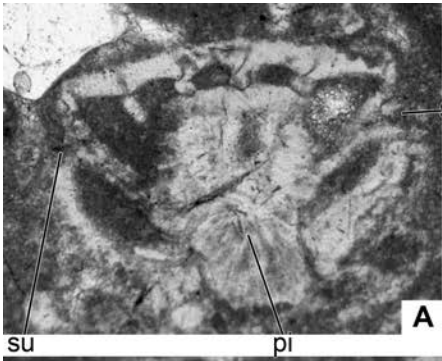
Small foraminifera	Nezzazzatinea sp.
Fleuryana sp.	Scandonea sp.
Dictyopsella kiliani	Cuneolina cylindrica
Indet. miliolids	Murgeina apula
Cuvillerinella cf. salentina	Murciella aff. cuvillieri
Praetorsella roestae	Pararotalia tuberculifera
Suturina minima sp. nov.	Suturina globosa
Rotalia baetica sp. nov.	Rotalispira scarsellai
Rotalinella sp.	Lepidorbitoides cf. socialis
Orbitoides cf. megaliformis	Praesiderolites douvillei
Pseudosiderolites vidali	Siderolites praecalcaripoides
Discorbids	Carophyte
Ostracod	





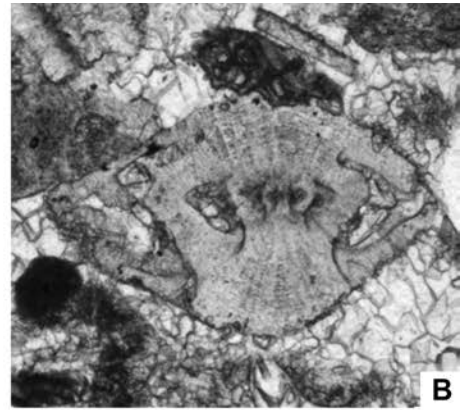








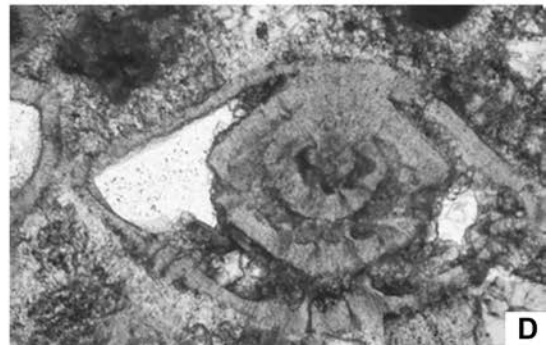
A



B



C



D

